ELEMENTA
Science of the Anthropocene

Parrington, M, et al. 2025. Biomass burning emission estimation in the MODIS era: State-of-the-art and future directions. *Elem Sci Anth*, 13: 1. DOI: https://doi.org/10.1525/elementa.2024.00089

REVIEW

Biomass burning emission estimation in the MODIS era: State-of-the-art and future directions

Mark Parrington[1,*], Cynthia H. Whaley[2], Nancy H. F. French[3], Rebecca R. Buchholz[4], Xiaohua Pan[5], Christine Wiedinmyer[6], Edward J. Hyer[7], Shobha Kondragunta[8], Johannes W. Kaiser[9], Enza Di Tomaso[1], Guido R. van der Werf[10], Mikhail Sofiev[11], Kelley C. Barsanti[4], Arlindo M. da Silva[5], Anton S. Darmenov[5], Wenfu Tang[4], Debora Griffin[12], Maximilien Desservettaz[13], Therese (Tess) Carter[14], Clare Paton-Walsh[13], Tianjia Liu[15], Andreas Uppstu[11], and Julia Palamarchuk[11]

Accurate estimates of biomass burning (BB) emissions are of great importance worldwide due to the impacts of these emissions on human health, ecosystems, air quality, and climate. Atmospheric modeling efforts to represent these impacts require BB emissions as a key input. This paper is presented by the Biomass Burning Uncertainty: Reactions, Emissions and Dynamics (BBURNED) activity of the International Global Atmospheric Chemistry project and largely based on a workshop held in November 2023. The paper reviews 9 of the BB emissions datasets widely used by the atmospheric chemistry community, all of which rely heavily on Moderate Resolution Imaging Spectroradiometer (MODIS) satellite observations of fires scheduled to be discontinued at the end of 2025. In this time of transition away from MODIS to new fire observations, such as those from the Visible Infrared Imaging Radiometer Suite (VIIRS) satellite instruments, we summarize the contemporary status of BB emissions estimation and provide recommendations on future developments. Development of global BB emissions datasets depends on vegetation datasets, emission factors, and assumptions of fire persistence and phase, all of which are highly uncertain with high degrees of variability and complexity and are continually evolving areas of research. As a result, BB emissions datasets can have differences on the order of factor 2–3, and no single dataset stands out as the best for all regions, species, and times. We summarize the methodologies and differences between BB emissions datasets. The workshop identified 5 key recommendations for future research directions for estimating BB emissions and quantifying the associated uncertainties: development and uptake of satellite burned area products from VIIRS and other instruments; mapping of fine scale heterogeneity in fuel type and condition; identification of spurious signal detections and information gaps in satellite fire radiative power products; regional modeling studies and comparison against existing datasets; and representation of the diurnal cycle and plume rise in BB emissions.

Keywords: Biomass burning, Emission estimation, Earth observation, Atmospheric composition

1. Introduction

Biomass burning (BB) emissions are of great importance worldwide due to their impacts on human health, ecosystems, air quality, and climate. All major atmospheric modeling efforts (e.g., models of atmospheric chemistry and transport, operational air quality forecast models, Earth-

[1] European Centre for Medium-Range Weather Forecasts, Bonn, Germany
[2] Climate Research Division, Environment and Climate Change Canada, Victoria, BC, Canada
[3] Michigan Tech Research Institute, Ann Arbor, MI, USA
[4] NSF National Center for Atmospheric Research, Boulder, CO, USA
[5] NASA Goddard Space Flight Center, Greenbelt, MD, USA
[6] CIRES, University of Colorado, Boulder, CO, USA
[7] Naval Research Laboratory, Monterey, CA, USA
[8] NOAA NESDIS Center for Satellite Applications and Research, College Park, MD, USA
[9] Klima- og miljøinstituttet NILU, Kjeller, Norway
[10] Meteorology and Air Quality Group, Wageningen University & Research, Wageningen, the Netherlands
[11] Finnish Meteorological Institute, Helsinki, Finland
[12] Air Quality Research Division, Environment and Climate Change Canada, Toronto, ON, Canada
[13] Environmental Futures, University of Wollongong, Wollongong, New South Wales, Australia
[14] George Washington University, Washington, DC, USA
[15] Department of Geography, University of British Columbia, Vancouver, BC, Canada

* Corresponding author:
Email: mark.parrington@ecmwf.int

Downloaded from http://online.ucpress.edu/elementa/article-pdf/13/1/00089/895115/elementa.2024.00089.pdf by guest on 29 September 2025

system models, etc.) require accurate estimates of BB emissions as a key input. Development of global BB emissions datasets relies on observations of active or recent fires, vegetation datasets and modeling, and emission factors (EFs; required to estimate the mass of smoke pollutant emitted per mass of fuel burned), all of which are highly uncertain and evolving fields of research. Current BB emissions datasets rely heavily on satellite observations, and in particular on observations of fire radiative power (FRP) and burned area from the Moderate Resolution Imaging Spectroradiometer (MODIS) instruments on the National Aeronautics and Space Administration (NASA) Terra and Aqua satellites. However, these observations will not be available for much longer as the orbits of the satellites degrade and are decommissioned at the end of 2025. The Visible Infrared Imaging Radiometer Suite (VIIRS) satellite instruments, on the joint NASA and National Oceanic and Atmospheric Administration (NOAA) Suomi National Polar-orbiting Partnership (Suomi NPP), NOAA-20, and NOAA-21 weather satellites, are currently the main replacement for the Aqua MODIS instrument. These instruments have an equator crossing time at around 1.30 PM/AM local solar time (LST) and therefore observe the typical afternoon peak in global BB activity (e.g., Mu et al., 2011; Andela et al., 2015). VIIRS has almost 4 times higher spatial resolution than MODIS, at 375 m compared to 1 km of MODIS at nadir. A burned area product has been developed for VIIRS based on the mapping approach derived from the most recent MODIS burned area algorithm (Giglio et al., 2024a) but has not yet been used by any of the BB emission datasets considered here. VIIRS does, however, offer other enhancements over MODIS such as the day–night band which allows for estimation of the visible energy fraction and modified combustion efficiency (MCE) at night (Zhou et al., 2023). Another relevant instrument is Sea and Land Surface Temperature Radiometer (SLSTR) on the European Sentinel-3 satellites, which has the same 1 km spatial resolution at nadir as MODIS and will replace the Terra MODIS observations during the late morning orbit at 10.30 AM/PM, but has experienced some difficulties with daytime fire registration and quantification. While the main peak in BB activity typically occurs during the afternoon, the nighttime observations are important for capturing the diurnal cycle, particularly in light of evidence of a weakening nighttime barrier in some parts of the world allowing wildfires to burn through the night (e.g., Balch et al., 2022). The Canadian WildFireSat mission (https://database.eohandbook.com/database/missionsummary.aspx?missionID=906) to be launched in the late 2020s will provide much needed measurements later in the afternoon and capture more of the diurnal cycle of BB activity (Hope et al., 2024).

With growing interest in BB emissions not only in the scientific community but also for the wider public, better understanding and quantification of the uncertainties is becoming more important. The International Global Atmospheric Chemistry (IGAC) project's sponsored activity on Biomass Burning Uncertainty: Reactions, Emissions and Dynamics (BBURNED; https://igacproject.org/activities/bburned) aims to better quantify the current understanding of the uncertainty and variability in BB emission estimation and to determine how to more accurately represent atmospheric chemistry resulting from fire. A virtual Fire Emissions Workshop (FEW 2023), organized by BBURNED, jointly with the Task Force on Hemispheric Transport of Air Pollution (HTAP), in November 2023, brought together BB emissions developers to present their methodologies, recent developments, and challenges/uncertainties, followed by researchers presenting on emissions intercomparisons, at both regional and global scales, and by species. This report provides a summary of the FEW 2023 workshop and the contemporary status of BB emissions estimation nearing the conclusion of the MODIS era and to provide an assessment on future developments.

2. Biomass burning observations and emissions estimation

2.1. Global biomass burning observation methods

Earth observation satellites are essential for timely measurements of the global distribution, relative scale, and growth of fires. The information that they provide, and their potential application, depend on the orbital configuration of the satellite, which leads to trade-offs in spatial resolution and temporal frequency further contributing to the complexity in estimating BB emission uncertainties. Satellites in a Sun-synchronous Low Earth Orbit (LEO), utilized by many sensors (i.e., MODIS, VIIRS, SLSTR), cross the equator at the same LST on each overpass, have a consistent repeat time, and provide finer spatial resolution measurements than satellites in geostationary orbit (GEO). Sensors on LEO satellites do not measure throughout the full possible diurnal fire cycle that can be captured with the high temporal resolution from GEO satellites, which have also been shown to be able to detect smaller fires (e.g., Soja et al., 2009). However, no single sensor is able to provide global coverage (e.g., Roberts et al., 2015; Wooster et al., 2015).

2.2. Fire types, vegetation, and distribution

Vegetation fires have always been a naturally occurring, and essential, component of the Earth system with a growing number of studies in the scientific literature quantifying the impact human activities have on fire occurrence around the world (e.g., Bowman et al., 2020; Jones et al., 2024). Vegetation fires can refer to many different fire types (e.g., forest fires, grass fires, crop fires) and intensities (e.g., high intensity crown fires and low intensity, or smoldering, peat fires).

The heterogeneity of vegetation globally means that the characteristics of fires and the resulting smoke will be different based on vegetation type along with human activities. **Figure 1** illustrates the fire types that global fire emissions datasets are typically aligned with. For global implementation, vegetation type and its distribution must be simplified and this map represents one means of representing what is inherently a complex and heterogeneous variety of the vegetation fuels that can burn under various conditions. The term fuel is used to represent the material (biomass) subject to burning and is made up of the live and dead vegetation found in the landscape (Prichard et al., 2024). Fuels serve as the foundation of what can potentially end up as smoke; they are highly variable

Downloaded from http://online.ucpress.edu/elementa/article-pdf/13/1/00089/895115/elementa.2024.00089.pdf by guest on 29 September 2025

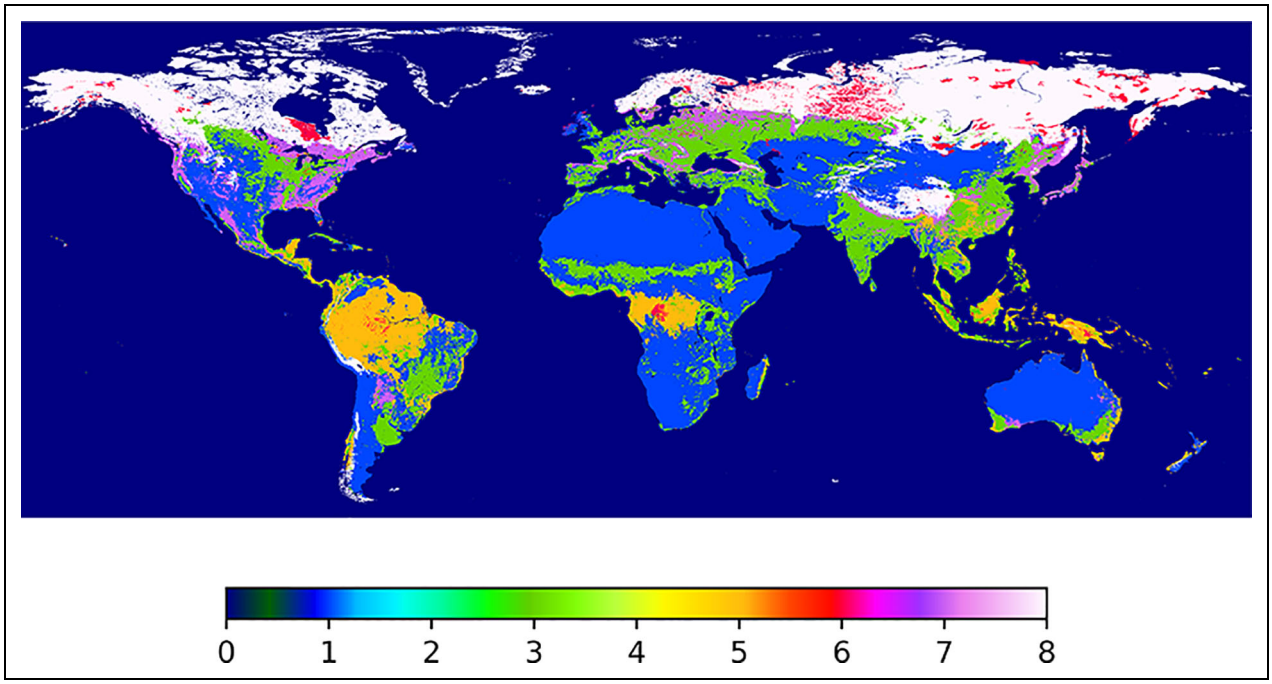

Figure 1. Dominant fire types extrapolated from van der Werf et al. (2010) in Kaiser et al. (2012) and adapted here for 2018 using ESA CCI Land Cover and Xu et al. (2018). 1 = savannah fires; 2 = savannah fires with potential soil organic matter burning; 3 = agricultural fires; 4 = agricultural fires with potential soil organic matter burning; 5 = tropical forest fires; 6 = peat burning; 7 = extra-tropical forest fires; 8 = extra-tropical forest fires with potential soil organic matter burning.

down to site-level scales and range from grasslands dominated by low-density herbaceous species to dense forests with large amounts of dead vegetation debris or deep organic soils which can hold as much as 1,000 Mg/ha or more of live and dead fuel, but with high temporal and spatial variability (Prichard et al., 2019).

2.3. Estimation of biomass burning emissions and smoke production

Combustion of biomass fuels produces energy (heat and light), gases, and solids of various sizes that are either left as residue at the site (ash and char) or lofted into the air. The process is fuels-driven and mediated by weather and topography to create spatial–temporal complexity in how and where fuels burn and the resulting emissions. A variety of different gaseous and particulate combustion products are emitted into the atmosphere depending on the fuel type and conditions during burning, including the fuel moisture, arrangement of fuels, terrain, and fire weather, which influence the intensity and efficiency of burning (Prichard et al., 2024).

Emissions of smoke from BB are estimated in a variety of ways to provide a consistent data record over space and time. Current regional and global inventory records begin in the 1980s using observations from satellite systems (Giglio et al., 2024b). Here we review the approaches used in global and continental-scale emissions estimation, including the methods reviewed for emissions systems covered in FEW 2023 (Section 3).

Emissions amount and composition (M_x) is calculated using an inventory approach from the total fuel consumed (M_c) in a specific place and emission factors (EF) of specific combustion products (x):

$$M_x = M_c \times \mathrm{EF}_x \quad (1)$$

Determination of both M_c and EF takes into consideration many factors, including the characteristics of the fuels and the conditions of the burn. Fuel type and condition are important in determining M_c as well as the combustion efficiency, which influences the composition of the smoke. EFs represent combustion efficiency to partition total fuel combusted into different smoke components and are explained in more detail in Section 2.4. Emissions inventories presented in this review employ one of the two approaches for determining the amount of biomass consumption for wildland fire (**Figure 2**). The first is the burn area approach (**Figure 2a**) used by the Global Fire Emissions Database (GFED) and the Fire INventory from NCAR (FINN). In this accounting-based approach, emissions are calculated from empirically derived models of consumption with estimates of the amount of area burned, the amount of fuel at the site, and fraction of that fuel that is converted to smoke (Seiler and Crutzen, 1980; Ottmar, 2014). The second is the combustion approach (**Figure 2b**), used by Quick Fire Emission Database (QFED), Global Biomass Burning Emissions Product eXtended (GBBEPx), and Global Fire Assimilation System (GFAS) datasets, which utilizes satellite-based observations of FRP from active fires and determines combustion level through empirically defined consumption factors (e.g., Wooster et al., 2005). Details on these activity-based approaches can be found in French and Hudak (2024).

Downloaded from http://online.ucpress.edu/elementa/article-pdf/13/1/00089/895115/elementa.2024.00089.pdf by guest on 29 September 2025

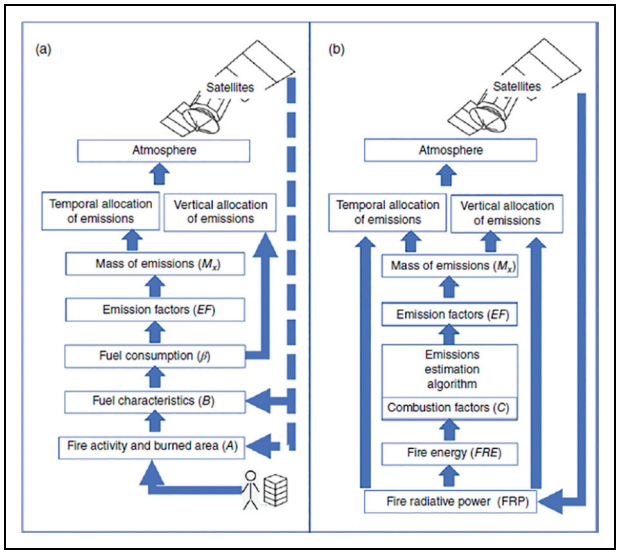

Figure 2. Two approaches to determine emissions from BB. (a) The burn area approach considers the amount of area burned (*A*), prefire fuels (*B*), and proportion of fuel consumed (β). (b) The combustion approach uses fire radiative energy (FRE) to estimate consumption based on fuel-type-specific combustion factors (*C*). An emission factor (EF) for each product is applied based on combustion conditions (French and Hudak, 2024).

The quality of BB emission estimation starts with the quality of the input fire observations, whether burn area or active fires, knowledge of the representative fuels related to the observation, and area. In mapping burn area, the basis for computing emissions for the burn area approach, and for calibrating the combustion approach, maps can be incomplete due to satellite coverage and because fire events can be obscured by clouds or forest canopies. Additionally, subsurface fires, such as those in peat lands, are not currently well detected by satellites and emissions can be underestimated. For FRP observations, false detections and spurious signals can arise from active volcanoes and bright surfaces, such as solar panels and shallow coastal waters at certain viewing angles, requiring screening of the raw thermal anomaly data. Gas flaring is also a source of spurious signals for BB emission estimation but FRP observations have been used in quantifying emissions from these activities (e.g., Caseiro et al., 2020).

The fuel availability, described in Section 2.2, and its associated variability are also critical components in estimating BB emissions. Both the amount and density of fuel (referred to as fuel loading) and the fuel condition, such as moisture and arrangement, contribute to the amount of fuel that is available to burn and what is actually consumed during combustion (combustion completeness). These factors introduce large spatial and temporal variability in emissions. Fuel heterogeneity represents one of the largest sources of uncertainty in any emissions estimation approach, while variability in combustion completeness adds to the high uncertainty in estimating emissions even when fuel type is known (French et al., 2004; Larkin et al., 2012). Use of fire energy estimates from observations in the combustion approach (right side of **Figure 2**) can capture some but not all of the combustion completeness variability and does not avoid the need for spatially resolved information on fuel types and fire regimes (e.g., Ichoku and Kaufman, 2005; Mota and Wooster, 2018). Development of methods to improve quantification and to characterize BB fuels is on-going (Bright et al., 2022; Cova et al., 2023) as well as ways to better map and quantify fuels and fuel consumption variability in space and time (Prichard et al., 2019; French et al., 2020; Kennedy et al., 2020).

2.4. Emission factors

EFs define the partitioning of combustion products into species-specific emissions, which are variable based on the fuel type and combustion conditions. In general, the more oxygenated the burning conditions (flaming vs. smoldering combustion), the more efficient the combustion and the more carbon dioxide (CO_2) is produced relative to other combustion products (Yokelson et al., 1996). BB EFs are determined by measuring the relative concentrations of pollutants from BB emissions (either from controlled burning in the laboratory/field or sometimes from aircraft campaigns measuring uncontrolled fires) (e.g., Yokelson et al., 1996; Yokelson et al., 2013; Urbanski et al., 2022). Seasonal and regional variability in EFs is an important source of uncertainty in BB emission estimation (e.g., Vernooij et al., 2023), and the uncertainty can depend on the scale at which EFs are applied. For global scale emissions inventories, specific EFs are applied by biome (e.g., Kaiser et al., 2012; van Leeuwen et al., 2014). EFs are dependent on the fuel type and combustion conditions (e.g., Prichard et al., 2020) and, therefore, can have a high degree of variability for event-based and regional BB emission estimation. Region-specific knowledge of EFs is often applied for air quality modeling efforts in different countries. This has been particularly the case for Australia where studies combining locally measured EFs and knowledge of indigenous cultural burning practices to provide more detailed information on country-specific BB emissions estimates (see Supplementary Material for more information).

Recent efforts to better characterize the composition of smoke for emissions modeling have resulted in several updates to EFs from BB and other open burning (Andreae, 2019; Prichard et al., 2020). The Andreae (2019) inventory includes EFs for 121 gas- and particle-phase species or constituents (i.e., total particulate matter, TPM). The data are almost entirely from field measurements and include a range of globally relevant fuel and fire types. The Smoke Emissions Repository Application (SERA) database (Prichard et al., 2020) includes EFs for 276 gas- and particle-phase species or constituents focused on North American wildland fuels including both laboratory and field data. The Next-generation Emissions InVentory expansion of Akagi database (NEIVA; Binte Shahid et al., 2024), described in Section 2.4.1, is similar to Andreae (2019), and includes EFs for globally relevant fuel and fire types, but covers over 800 compounds and representative laboratory data were selectively included. As with

Downloaded from http://online.ucpress.edu/elementa/article-pdf/13/1/00089/895115/elementa.2024.00089.pdf by guest on 29 September 2025

SERA, NEIVA is an online, searchable database. The EFs in these databases are generally used as static inputs to models even though they are dependent on the stage of combustion (e.g., flaming vs. smoldering). With the emergence in recent years of space-based estimates of MCE, efforts are under way to establish acceptable assumptions of these effects on EFs for general use (e.g., Zhou et al., 2023).

2.4.1. NEIVA

The NEIVA database (NEIVA; Binte Shahid et al., 2024) is a new database in which the EFs for 14 globally relevant fuel and fire types have been updated to include data from recent studies, with a focus on gaseous non-methane organic compounds (NMOC_g, where g denotes gaseous emissions). In v1.0, NEIVA exists as a collection of datasets and Python script files, all of which are available through the NEIVA GitHub site (https://github.com/NEIVA-BB-Emissions-Inventory). The datasets include a primary database with collected and reformatted data from: existing emission inventories (e.g., Akagi et al., 2011 and updates; Andreae, 2019); recent laboratory and field campaigns compiled from 30 publications (2015 and later); a recommended EF dataset with EFs averaged across studies and summarized for the 14 fuel and fire types.

Additional features of NEIVA include a property dataset that links each NMOC_g with a suite of chemical and physical properties using unique identifiers; NMOC_g are mapped to SAPRC, MOZART-T1, and GEOS-Chem model surrogates to facilitate inclusion of recent data in model applications; EFs for inorganic gases and particulate matter (PM) constituents (e.g., elemental carbon, organic carbon, water soluble organic carbon, ions); and flexible querying across datasets (that represent different levels of processing, merging, and averaging) that allow EF retrieval from the individual study level to averaged across all studies for a given fuel or fire type, and from the individual compound or constituent level to representative model surrogate species.

The number of NMOC_g represented in NEIVA is up to an order of magnitude higher than in the most recent EF compilations. Inclusion of this more diverse set of NMOC_g changes property distributions, for example, the volatility distribution and OH reactivity (OHR) of the represented compounds, that can affect predictions of atmospheric composition and chemistry. Mapping this more diverse set of NMOC_g to model surrogates also leads to distinct differences in the surrogate distributions when compared with other existing compilations that are likely to affect multiscale model predictions. NEIVA has a better representation of intermediate volatility compounds, resulting in a shift in the volatility distribution to lower volatilities, with the lowest volatility bin shifted by up to 3 orders of magnitude. In addition, the NEIVA NMOC_g speciation profiles when mapped to SAPRC-07 model surrogates resulted in higher OHR by 40%–90% (Binte Shahid et al., 2024).

3. Emissions datasets

Each emission dataset is described in a sub-section below, and its characteristics summarized in **Table 1**.

Table 1. Summary of global BB emissions datasets[a]

Dataset	Sensor Product	Approach	Resolution	NRT	Aerosol Scaling	Peat Fire Emissions	Main Use
GFEDv4s	MODIS burned area, active fire geolocations	Burn area	0.25˚	No	No	Yes for tropical peatlands	A
GFEDv5	MODIS burned area, MODIS and VIIRS active fires	Burn area	0.25˚	Yes	No	Yes	A
QFEDv2.5	MODIS and VIIRS Fire Radiative Power (FRP)	Combustion	0.1˚	Yes	Yes	No	A, B
GBBEPx	VIIRS FRP	Combustion	0.1˚	Yes	Yes	No	B
GFASv1.2	MODIS FRP	Combustion	0.1˚	Yes	No	Yes	A, B
FEERv1.0	MODIS FRP	Combustion	0.1˚	No	Yes	No	A
FINNv2.5	MODIS and VIIRS active fire geolocations	Burn area	1 km	Yes	No	No	A, B
FLAMBE	MODIS active fire geolocations	Burn area	1–3 km	Yes	Yes	No	B
IS4FIRES	MODIS FRP	Combustion	0.1˚	Yes	Yes	No	A, B

[a]Approach refers to the use of the burn area or combustion approaches, described in Section 2.3, to estimate emissions. NRT refers to near-real-time availability of the data required for operational smoke and air quality forecasts. Aerosol scaling refers to tuning of output emissions based on regional or other empirically derived factors for model applications. Peat fire emissions indicate if specific BB emissions for peatlands are available in the dataset. The main use of these datasets has been to provide publicly available long-term datasets better understanding long-term changes in global BB (labeled A in the table) and for operational air quality and atmospheric composition forecasts (labeled B in the table).

Downloaded from http://online.ucpress.edu/elementa/article-pdf/13/1/00089/895115/elementa.2024.00089.pdf by guest on 29 September 2025

3.1. GFED

The Global Fire Emissions Database (GFED) computes fire emissions based on the Seiler and Crutzen (1980) equation; multiplying satellite-derived burned area with modeled fuel consumption. Currently GFED version 4 (GFED4) with the addition of small fires (GFED4s) uses MODIS burned area collection 5 (Giglio et al., 2013) and small fire burned area based on statistical relations between MODIS active fire detections inside mapped burn scars (Randerson et al., 2012). Burned area is then multiplied by fuel consumption, which is modeled and varies spatially and temporally (van der Werf et al., 2017).

Over the course of 2025 GFED will transition to version 5 (GFED5), providing a major overhaul, and is expected to be released later in 2025, but a Beta version is currently available. GFED5 is based on the MODIS collection 6 burned area product (Giglio et al., 2018), and the small fire burned area detection algorithm has benefited from the use of Landsat and Sentinel-2 burn area information to better constrain the algorithm (Chen et al., 2023). Fuel consumption is based on van Wees et al. (2022) who ran a simplified GFED fuel model at native MODIS resolution. This allowed for improved calibration with field-derived fuel consumption. EFs are based on NEIVA (Section 2.4.1) and dynamic EFs for savannas from Vernooij et al. (2023).

The purpose of the dataset is to provide a publicly available, relatively long-term, retrospective, and consistent source of information to understand the role of fires in the global carbon cycle and climate system. The GFED4 dataset covers the 1997–2024 period, with the pre-MODIS era being based on Visible and Infrared Scanner (Giglio et al., 2000) and Along-Track Scanning Radiometer (Eva and Lambin, 1998) satellite observations, and post-2016 emissions are derived from grid-cell-specific relations between emissions and MODIS active fires for the 2001–2016 overlapping period. GFED5 covers the 1997–now period, the post-2022 period will be based on VIIRS active fire detections scaled to GFED5 emissions. The spatial resolution of the GFED datasets is 0.25°, the temporal resolution is monthly and uses scalars to convert monthly data to daily or 3-hourly timesteps. The EFs used are mostly derived from Akagi et al. (2011).

GFED4s data are publicly available with a delay of approximately 1 year. However, the use of VIIRS active fire detections used in GFED5 will provide near-real-time (NRT) availability. More information can be found on http://www.globalfiredata.org/.

3.2. QFED

The Quick Fire Emissions Dataset (QFED) (Darmenov and da Silva, 2015) uses an approach based on MODIS and VIIRS FRP observations to calculate gridded daily fire emissions and daily mean gridded FRP for each satellite instrument and biome. BB emission estimation with QFED is based on 4 global biomes (tropical forest, extratropical forest, savanna, and grassland), which is an aggregate of the International Geosphere–Biosphere Programme (IGBP) land cover classes. Calibration of BB emissions for trace gases and aerosols is made in 2 ways. For trace gases, GFED-based calibration is performed for carbon monoxide (CO), and emissions of the other species are derived based on the ratio of EFs. For aerosols, QFED is intended as a *perceived emission dataset*; that is, the emissions that initialize smoke in the GEOS model are needed to simulate realistic aerosol optical depth (AOD) distributions in the atmosphere. Calibration coefficients for each biome are obtained through an inverse calculation constrained by MODIS AOD observations retrieved using Global Modeling and Assimilation Office's Neural Net Retrieval trained on AERONET data.

In preparation for the end of the MODIS era, QFED developments are planned to use FRP observations from geostationary satellites to capture the diurnal cycle in emissions. Additional future developments for QFED include the adoption of the biomes, including peatlands, provided by the NASA FIre Light Detection Algorithm (FILDA; Zhou et al., 2023) and to implement MCE calculations to modulate EFs using nighttime and daytime distributions. A Bayesian multispectral, biphasic algorithm is being developed to provide separate estimates of the flaming and smoldering/residual components of FRP, alongside associated heat fluxes. These capabilities permit the specification of combustion phase dependent EFs, and when combined with the thermodynamic environment, the estimation of vertical mass distribution functions using plume rise models such as Freitas et al. (2010).

QFED is operated in NRT and in delayed (reanalysis) mode by the NASA GMAO. QFED provides emissions for the aerosol, greenhouse, and reactive gases components for the GEOS Earth System model and is the foundation for GMAO reanalyses, mid-range, sub-seasonal, and seasonal forecasting systems.

Currently, QFED provides gridded emissions products at 25 and 10 km nominal resolution with a latency of approximately 6-h after 00 UTC for NRT, and approximately 1 week for "science quality" data. The dataset covers the full MODIS period with VIIRS starting in 2012. The data are publicly available on request from NASA GMAO.

3.3. GBBEPx and RAVE

The current operational Global Biomass Burning Emissions Product eXtended (GBBEPx) V5 algorithm estimates fire emissions from VIIRS 375m FRP observations aggregated by biome type (tropical forest, extratropical forest, savanna, and grassland) to a 0.05° grid cell. Initial versions of the GBBEPx algorithm were applied to MODIS and VIIRS observations, GBBEPx phased out MODIS and currently uses only VIIRS instruments on the NOAA-20 and NOAA-21 satellites.

FRP density for a predefined grid (e.g., $0.1^\circ \times 0.1^\circ$) is calculated by remapping individual VIIRS active fire observations. Emissions are estimated using regression parameters derived by correlating VIIRS FRP density with QFED V2.5 emissions stratified into different biome types for each continent. The reliance on QFED V2.5 to derive GBBEPx emissions requires regression parameter updates whenever QFED undergoes a revision. NOAA is planning to completely modify its emissions algorithm to use

Downloaded from http://online.ucpress.edu/elementa/article-pdf/13/1/00089/895115/elementa.2024.00089.pdf by guest on 29 September 2025

merged polar-orbiting and geostationary satellites using its newly developed algorithm (see Li et al., 2022).

NOAA has also developed a new operational algorithm (Li et al., 2021), Regional hourly Advanced Baseline Imager and Visible Infrared Imaging Radiometer Suite Emissions (RAVE), to generate regional hourly 3 km fire emissions across North America using a combination of FRP observations from the Advanced Baseline Imager (ABI) on the Geostationary Operational Environmental Satellites–R Series (GOES-R) and VIIRS. High temporal resolution of ABI allows for characterizing fires and emissions on a diurnal scale. The RAVE algorithm calibrates and fuses the ABI FRP with VIIRS FRP in 3 km grids. FRP diurnal cycles at an interval of 5 min are reconstructed using the fused ABI-VIIRS FRP combined with the land cover-ecoregion-specific FRP diurnal climatologies. The reconstructed FRP diurnal cycles are applied to estimate hourly emissions of 10 species (e.g., CO and fine PM with diameters < 2.5 μm ($PM_{2.5}$)). The RAVE algorithm is expanding to use geostationary FRP observations covering Europe and Asia.

Daily GBBEPx emissions are currently used by the NOAA National Weather Service in its operational global aerosol model (Zhang et al., 2022). Hourly RAVE emissions data are operationally used by the National Weather Service regional air quality forecast model. NOAA currently has processed the entire VIIRS record from 2012 to the present and the datasets on a 0.25° × 0.25° grid resolution that are made available to users by request. Operational GBBEPx data with a 1-day latency are publicly available for download at https://www.ospo.noaa.gov/products/land/gbbepx/, and operational RAVE data with a 2-h latency are publicly available for download at https://www.ospo.noaa.gov/products/land/rave/.

3.4. GFAS

The Global Fire Assimilation System (GFAS) computes fire emissions in NRT from satellite observations of FRP and assumptions dependent on vegetation type (Kaiser et al., 2009; Kaiser et al., 2012). GFAS version 1.2 (GFASv1.2) is based on FRP observations from the MODIS instruments on the Terra and Aqua satellites (Giglio et al., 2016) to calculate emission rates of various smoke constituents using static EFs from Andreae and Merlet (2001) and Christian et al. (2003). These calculations of combustion rate and species emissions contain representations of peat in Southeast Asia and Siberia.

Spurious signals, for example, from gas flaring, powerplants, and volcanic outflow, are masked with a static map and the combustion rate is calculated from FRP (following Wooster et al., 2005) currently using 8 empirical factors for 8 different land cover types, which have been derived from a regression against the combustion rate of GFED3 (van der Werf et al., 2010; Kaiser et al., 2012). Furthermore, the GFAS algorithm applies a solution for partial observational cloud coverage, taking into account observation representativity errors as well as observation uncertainty due to satellite sensor detection limits to estimate a GFAS analysis of FRP where observations are combined with previous day analysis (or first-guess) using a Kalman filter approach.

An updated, higher (hourly) temporal resolution version, GFASv1.4, also based on MODIS FRP observations, is already deployed in Copernicus Atmosphere Monitoring Service (CAMS) operational forecasts and planned to be released in the near future. The higher temporal resolution is achieved by assimilating daytime and nighttime FRP separately and superimposing a climatological diurnal cycle. Future updates to GFAS will assimilate FRP observations from the VIIRS instrument on the Suomi-NPP, NOAA-20, and NOAA-21 satellites (Csiszar et al., 2014) and from the geostationary Meteosat, GOES-E, GOES-W, and Himawari satellites to ensure the post-MODIS continuation of the dataset. Furthermore, dynamical bias correction, a machine learning-based FRP model, and EF updates are planned to contribute to GFAS improvements.

GFAS is operated in NRT by the European Centre for Medium-Range Weather Forecasts (ECMWF) as part of CAMS and used as input, with persistence, for operational forecasts, reanalysis, and other services provided by CAMS, as well as being publicly disseminated as an open access dataset. More information, and data access, is available from https://atmosphere.copernicus.eu/. The data are provided at a 0.1° spatial resolution for the period 2003 to present day, to cover the combined availability of both MODIS instruments. The data are publicly available 1-day behind (GFASv1.2) and 7-h behind (GFASv1.4) real time. GFASv1.2 is currently distributed via https://ads.atmosphere.copernicus.eu/datasets/cams-global-fire-emissions-gfas?tab=overview and GFASv1.4 data will also be distributed from there during 2025.

3.5. FEER

The Fire Energetics and Emissions Research (FEER) version 1.0 developed a global BB emissions dataset for various particle and trace gas species using the combustion approach (Ichoku and Ellison, 2014). Initially, FEER generated a global gridded map of emission coefficients (Ce) for smoke TPM by leveraging simultaneous measurements of FRP from the GFAS product (Kaiser et al., 2012), AOD from the MODIS sensors on the Terra and Aqua satellites, and wind vector data from the NASA Modern-Era Retrospective analysis for Research and Applications, Version 1 (MERRA) (Ichoku et al., 2008). Subsequently, the smoke TPM is calculated by multiplying Ce by time-integrated FRP. Finally, EFs are used to convert TPM emission estimates into the various species included in the FEERv1.0 emissions inventory. These EFs are derived from Andreae and Merlet (2001), with updates provided by Andreae (2019). The FEERv1.0 dataset for various particle and trace gas species between 2003 and 2013 is available from https://science.gsfc.nasa.gov/feer/.

3.6. FINN

The Fire INventory from NCAR (FINN) is a model framework that produces global, daily fire emissions estimates at an approximate 1 km^2 horizontal resolution (Wiedinmyer et al., 2011; Wiedinmyer et al., 2023). The

Downloaded from http://online.ucpress.edu/elementa/article-pdf/13/1/00089/895115/elementa.2024.00089.pdf by guest on 29 September 2025

model uses the Seiler and Crutzen (1980) equation (burn area method), assuming that the emissions are a function of burned area, fuel loading, fuel consumption, and EF. The FINN framework estimates burned area from satellite-derived fire detections and satellite-derived vegetation inputs with estimates of fuel loading and EFs reported from field and laboratory studies.

The most recent version of FINN, version 2.5 (FINNv2.5), enables simultaneous use of multiple satellite products for emissions estimates. Currently, MODIS Collection 6 (MCD14DL) active fire detections and VIIRS active fire products obtained from NASA's Fire Information for Resource Management System data portal can be applied: one or both products may be used. Land Cover is assigned by year from the MODIS LCT MCD12Q1 Version 6 Land Cover Type Product with the IGBP classification scheme and the MODIS MOD44B v006 MODIS/Terra Vegetation Continuous Fields annual product. FINNv2.5 includes a preprocessor and an emissions module, all openly accessible (Wiedinmyer et al., 2023). Within the FINNv2.5 preprocessor, fire detections are spatially processed to produce estimates of burn areas and overlaid onto the vegetation information.

FINN BB emissions are used in applications including forecasting in the NCAR Whole Atmosphere Community Climate Model (WACCM), and retrospective model analyses.

Emission estimates are available from 2002 to the present day (Wiedinmyer and Emmons, 2022) at a spatial resolution of 1 km and daily temporal resolution. The emissions are available in NRT and the data are publicly available from https://www2.acom.ucar.edu/modeling/finn-fire-inventory-ncar.

3.7. FLAMBE

The Fire Locating and Monitoring of Burning Emissions (FLAMBE) system generates satellite-based estimates of spatially and temporally resolved emissions of PM in NRT (Reid et al., 2009). It has been used to supply emissions estimation for operational smoke predictions from the Navy Aerosol Analysis and Prediction System (NAAPS) since 2007. FLAMBE was originally developed to utilize the fire detections from GOES imagers provided by the Wildfire Automated Biomass Burning Algorithm (Prins and Menzel, 1994), and it currently uses the MODIS MOD14 thermal anomaly product, Collection 6.1 (Giglio et al., 2016) to calculate burn area.

FLAMBE does not use MODIS FRP, relying instead on scaling hot spots to burned area according to land cover classification (burn area approach). Fuel loading, fuel consumption, and EFs are derived from field observations (e.g., Reid et al., 2005a; Reid et al., 2005b) and similarly assigned based on land cover.

Applications of FLAMBE have typically applied regional scaling factors to improve the realism of outputs from specific chemical and aerosol transport models (e.g., GEOS-Chem in Fisher et al., 2010; NAAPS in Hyer and Chew, 2010; and WRF-Chem in Wang et al., 2013). Lynch et al. (2016) applied both a regional scaling of FLAMBE emissions and a temporal filter to mitigate day-to-day shifts in the orbital pattern (Heald et al., 2003). Forecasting using FLAMBE emissions is done with persistence, although some testing of dynamic emissions has been done (Peterson et al., 2013).

The design of FLAMBE reflects the goals of low latency for NRT operations, traceability to field measurements, and simplicity. FLAMBE emissions are a means to include spatially and temporally resolved BB emissions in atmospheric models, but they are not constrained to balance with other components of the carbon cycle and thus are not suited for most climate research applications.

FLAMBE provides emissions in a vector form, with emissions assigned at the locations of observed satellite hot spots; this is done to maximize consistency between simulations from models with different horizontal grids. Hourly emissions are estimated by applying land-cover-dependent diurnal cycles derived from geostationary fire observations (Reid et al., 2004).

Consistently processed FLAMBE emissions datasets are available for 2002–2022 and can be obtained from the Global Ocean Data Assimilation Experiment (GODAE; https://usgodae.org/cgi-bin/datalist.pl?dset=nrl_7seas&summary=Go). GODAE also includes some additional documentation of the FLAMBE data products.

3.8. IS4FIRES

The emission inventory produced by Integrated System for vegetation fires, IS4FIRES (http://is4fires.fmi.fi), is computed from MODIS FRP using the combustion approach: emission of gases and aerosols is calculated directly from FRP using empirical EFs (Sofiev et al., 2009; Soares et al., 2015). The IS4FIRES system is operated by Finnish Meteorological Institute in close connection with the System for Integrated modeLling of Atmospheric coMposition (SILAM; http://silam.fmi.fi) and used as inputs to forecast and hindcast of atmospheric composition, air quality, data for impact assessment studies, and so on (Romanello et al., 2023; Chowdhury et al., 2024; Curto et al., 2024).

The approach relies on the linear relation between the FRP and a rate of the biomass consumption (Mota and Wooster, 2018; Nguyen et al., 2023) and uses inverse dispersion modeling to identify these factors.

The inventory is based on 2 primary EFs converting FRP to total-PM and CO, which are obtained via inversion performed with SILAM. The EFs for PM are inferred from an iterative fitting of SILAM-calculated AOD with the corresponding Aeronet and MODIS AOD observations. The EFs for CO are based on a similar calibration procedure with Measurements Of Pollution In The Troposphere (MOPITT) retrievals: CO column and vertical profiles. The EFs distinguish between the continents and 7 land-use classes in each continent (in total, 34 nontrivial land-use categories). Each land-use category has its own EF from FRP to PM and from FRP to CO, that is, the fitting has 68 factors to identify from an inverse-problem solution. To constrain this multidimensional problem, the emission inversion is performed over a time period of 3–5 years. The total-PM and CO emissions are used as proxies for

Downloaded from http://online.ucpress.edu/elementa/article-pdf/13/1/00089/895115/elementa.2024.00089.pdf by guest on 29 September 2025

multicomponent emissions supplied to SILAM. EFs for the other emitted species are taken from Akagi et al. (2011).

Conversion of instant MODIS FRP observations into hourly emission fluxes involves the diurnal variation obtained from FRP retrievals from the SEVIRI geostationary satellite over Africa, also covering Europe (Soares et al., 2015). The obtained diurnal variation is extended to other continents using multiannual MODIS FRP data: the shape of the variation is kept but the absolute variation is scaled according to the MODIS day–night FRP ratio. The emission inversion depends on the features of the plume dispersion; therefore, attention was given to the plume elevation, for which the semiempirical formula has been derived using MISR active fire and plumes datasets (Sofiev et al., 2012; Sofiev et al., 2013).

At the global scale, IS4FIRES BB emissions are provided with a spatial resolution 0.1° and 1 h time resolution.

The current IS4FIRES v.2.0 is operated in NRT with the data open at the SILAM data portal http://silam.fmi.fi/thredds. The portal also contains the archive starting from the beginning of MODIS observations in 2000. The historical fire-induced smoke concentrations are openly available from an online data archive (Hänninen et al., 2024).

4. Intercomparison and known differences

Direct evaluation of global BB emissions is challenging due to highly limited availability of independent measurements (especially from satellites) and the heterogeneous spatial and temporal distribution of BB activity. However, indirect evaluation is possible through intercomparison of different BB emissions inventories, as well as by using these inventories in chemical transport models and evaluating the resulting modeled smoke against satellite observations and in situ measurements. Evaluation against satellite observations has typically occurred for CO, nitrogen dioxide (NO_2), and AOD; although formaldehyde (HCHO) and some other species are also possible. Several emission intercomparison studies have revealed large differences in BB emissions by species and by region. There have also been several studies that applied the different emissions in the same model in order to evaluate the results against measurements. This section summarizes the important findings in those studies, first globally (Section 4.1), and then by region (Section 4.2).

4.1. Global

Fire emissions from several inventories have been compared by Wiedinmyer et al. (2023), namely FINNv2.5 (MODIS+VIIRS), FINNv2.5 (MODIS), GFED4s, FEER, GFAS, and QFED. Global and regional comparisons for 2012–2019 highlight the complexity in evaluating BB emissions, with varied results across inventories for different species in different regions (**Figure 3**). In general, the year-to-year variabilities in the annual fire emissions are consistent between different inventories, however the magnitudes of the emissions differ. The 2 inventories predicting the highest global emissions of CO_2 and CO were FINNv2.5 with MODIS+VIIRS and FEER. These inventories estimated approximately double the emissions of CO_2 and CO, compared to GFED4s, QFED, GFAS, and FINNv1.5. However, these inventory differences are not conserved across different species. Species variability is indicated by, for example, QFED producing the lowest global HCHO emissions but highest global black carbon (BC) + organic carbon (OC) emissions, compared to the other inventories. Additionally, these estimates vary regionally. For example, FINNv2.5 (MODIS+VIIRS) has significantly higher emissions over Southeast Asia in spring than other inventories. In contrast, GFED4s and GFAS have higher emissions than other inventories over Boreal North America and Equatorial Asia in summer, likely due to the inclusion of peat fire emissions. Targeted measurements, such as the recent Airborne and Satellite Investigation of Asian Air Quality (ASIA-AQ) field campaign in early 2025, will help understand Southeast Asia BB emission inventory accuracy.

Griffin et al. (2024) compared CO emissions estimates from fires with satellite-derived CO emissions worldwide. They used high-resolution satellite data from the Tropospheric Monitoring Instrument (TROPOMI) to estimate CO emissions from individual fires globally between 2019 and 2021. As a first step, CO BB emissions were estimated directly from the satellite observations using a flux method, where the total mass of the CO enhancement is estimated from the satellite column observations averaged in 4 km boxes upwind and downwind across the fire entire plume, combined with ERA5 winds to determine an emission rate. As a next step, by combining these estimates with satellite FRP data from MODIS, they developed biome-specific emission coefficients and created annual CO BB emissions. Combining these TROPOMI-MODIS derived emission coefficients and total MODIS FRP (such as the GFAS FRP), total emissions annual CO emissions were derived. They found that Southern Hemisphere Africa had the highest CO emissions from BB, accounting for over 25% of the global total of 300–390 Mt(CO)/yr from 2003 to 2021, in terms of biomes: broad-leaved evergreen tree fires contributing almost 25% of global emissions. The study also compared different BB CO emission inventories (including the Global Forest Fire Emissions Prediction System [GFFEPS; Anderson et al., 2024], GFED4.1, FINN1.5, FINN2.5, and GFAS) to the TROPOMI-MODIS total emissions (**Figure 4a**). The average global annual CO emissions from wildfires are roughly between 300 and 400 Mt/yr for all inventories except FINN2.5 inventory reported CO emissions on the order of 500–700 Mt/yr, consistent with Wiedinmyer et al. (2023). Over the past 2 decades, the satellite-derived global CO BB emissions have generally decreased by 5.1–8.7 Mt(CO)/yr, this decrease is driven by decreasing wildfire emissions from Africa and South America, however, the Temperate Forest North America (TENA) shows increasing emissions (Griffin et al., 2024; **Figure 4b**).

The fire emissions of aerosols from 6 global biomass burning emission datasets (i.e., QFED2.4, FEER1.0, FINN1.5, GFED3.1, and GFED4s) have been intercompared by Pan et al. (2020). In most regions worldwide, QFED2.4 and FEER1.0 datasets based on FRP have significantly more OC BB emissions than other datasets (**Figure 5a**). Averaged globally, QFED2.4 has a factor of 3.8 more OC emissions than GFED 4s, which has the least. Using the

Downloaded from http://online.ucpress.edu/elementa/article-pdf/13/1/00089/895115/elementa.2024.00089.pdf by guest on 29 September 2025

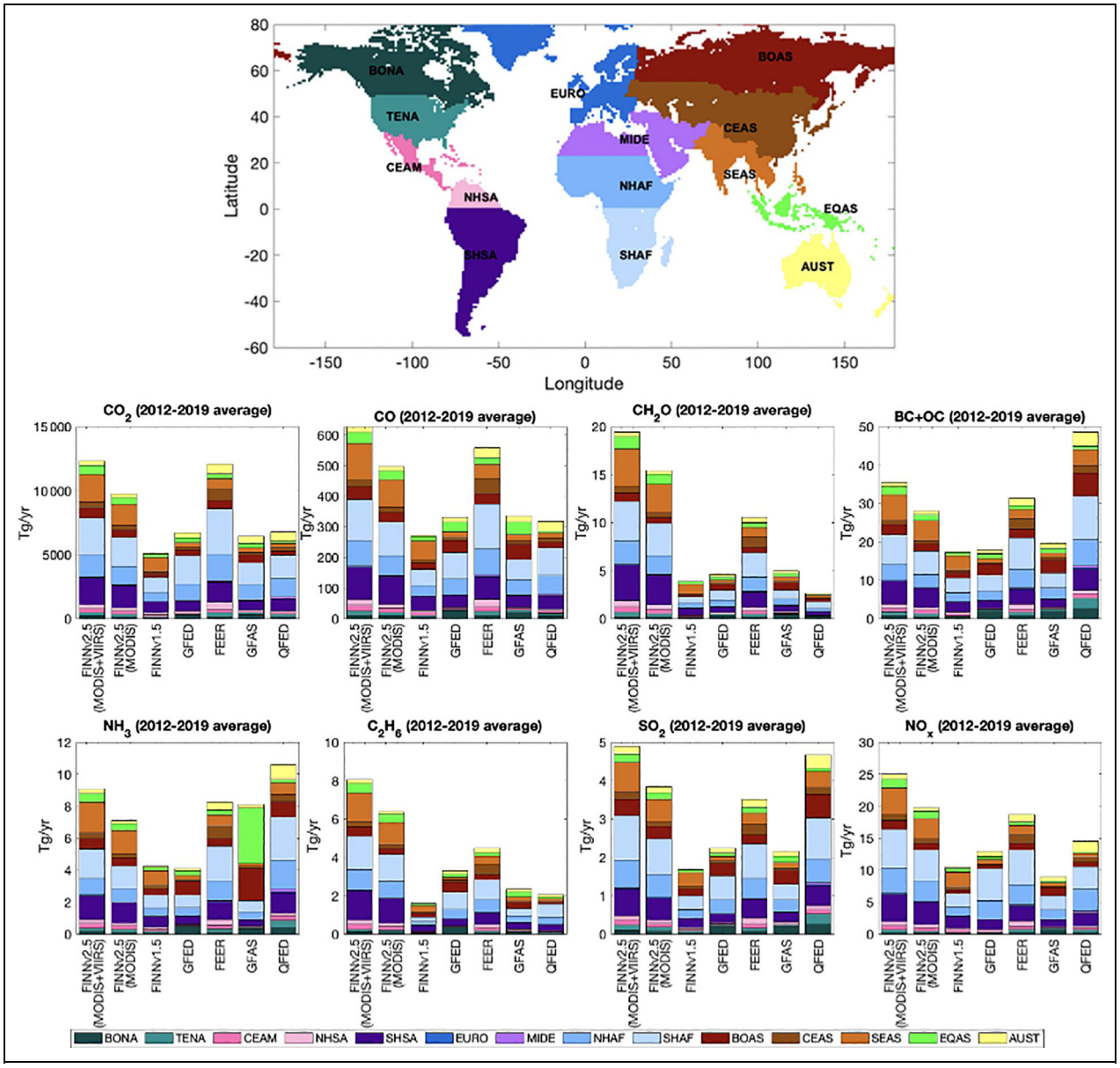

Figure 3. Intercomparison of several BB emissions datasets for several species and regions. Figure from Wiedinmyer et al. (2023, corrigendum).

NASA Goddard Earth Observing System (GEOS) model, simulated AODs with the QFED2.4 and FEER1.0 datasets are closest to the observed AOD from MISR and AERONET in the southern hemisphere when and where biomass burning emissions dominate (**Figure 5b**). In contrast, simulated AOD with GFED4s was underestimated most. Both QFED2.4 and FEER1.0 are based on FRP and constrain the emission coefficients used to derive BB aerosol emissions based on MODIS AOD. However, this constraint does not apply to other BB emission datasets.

4.2. Regional

Other research has had a more regional focus for evaluating fire emission estimates and their impact on air quality and climate modeling. For example, Carter et al. (2020) focused on North America within a global context using 4 commonly used smoke inventories (GFED4s, FINN1.5, GFASv1.2, and QFED2.4), a chemical transport model (GEOS-Chem), and observations from surface networks, aircraft, and satellites. They found that the 4 inventories perform differently depending on emitted species, location, and season (e.g., **Figure 6**). They also calculated that average BC and OC emissions differ by roughly a factor of 5 and 4, respectively, across the inventories in boreal North America. The range in BC and OC emissions in the contiguous United States is even larger (a factor of approximately 7 and 6, respectively). Global ranges in BC emissions are smaller than those in North America (approximately 2.3) with a somewhat more modest spread (approximately 1.7) in OC emissions, possibly because of EF differences. They also demonstrated that dry matter, not EF, differences are the driving force for emissions variation across inventories. Carter et al. (2020) showed that 2 of the inventories (GFED4s and GFASv1.2) lead to a better agreement between the model and observations in North America (**Figure 6**). While

Downloaded from http://online.ucpress.edu/elementa/article-pdf/13/1/00089/895115/elementa.2024.00089.pdf by guest on 29 September 2025

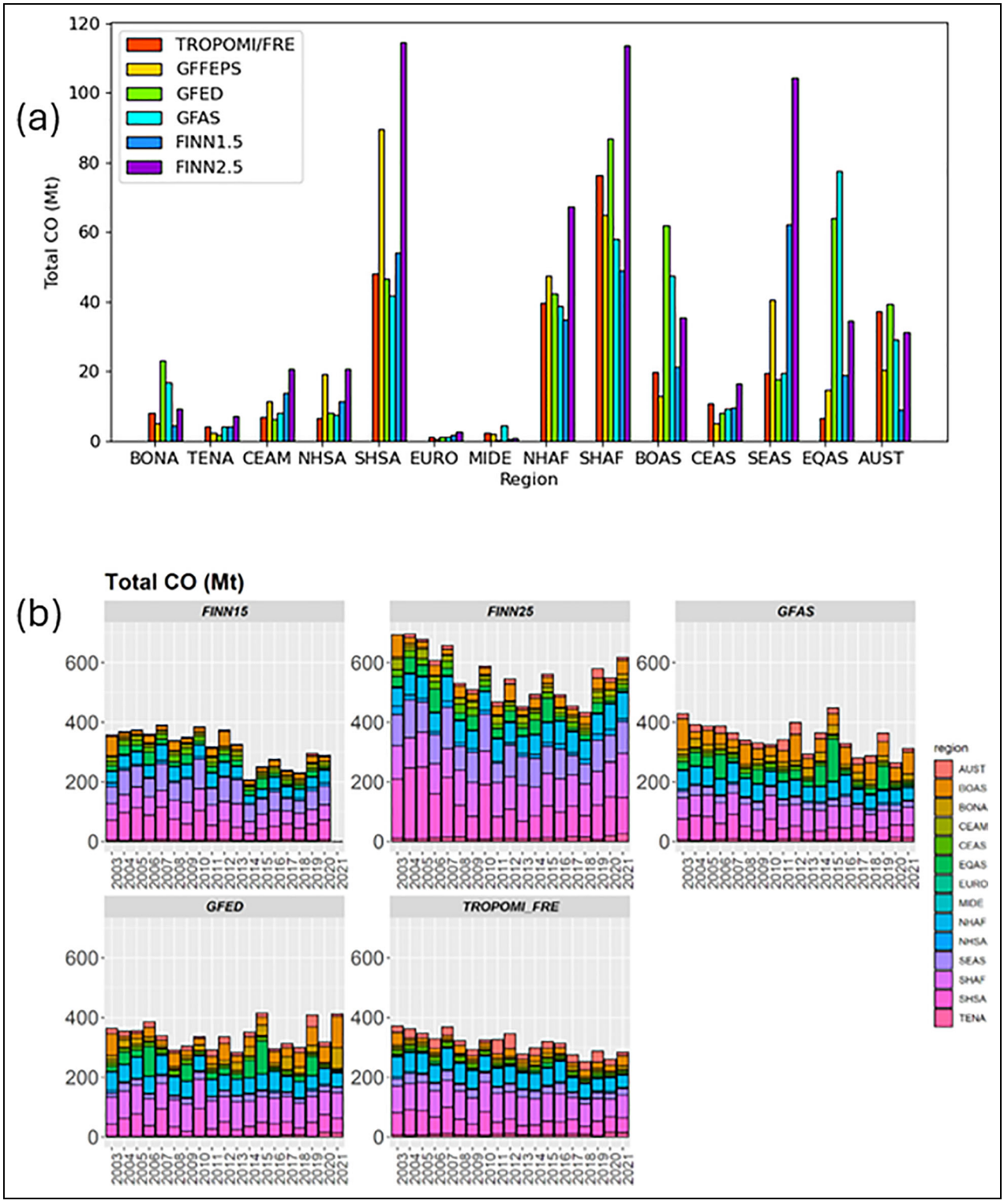

Figure 4. Intercomparison of several BB CO emission inventories compared to those derived from satellite measurements. (a) Regional annual totals for 2019 and (b) regional annual totals 2003–2021. Figure adapted from Griffin et al. (2024).

most air quality and climate studies only use one smoke inventory, they find that there is a large range across the inventories in health-relevant surface smoke concentrations and climate-relevant direct radiative effects. Tang et al. (2022) found for the Western United States, modeled CO and AOD using FINNv2.5 inputs to compare well with MOPITT CO and MODIS AOD. However, similar evaluations in other parts of the world suggested that FINN estimates of CO are overestimated in the Amazon basin and in central Africa.

Liu et al. (2020a) intercompared fire emissions in Indonesia for GFED4s, FINN1.5, QFED2.5r1, GFASv1.2, and FEER1.0-G1.2 and modeled surface smoke concentrations across Equatorial Asia (Indonesia, Malaysia, and

Downloaded from http://online.ucpress.edu/elementa/article-pdf/13/1/00089/895115/elementa.2024.00089.pdf by guest on 29 September 2025

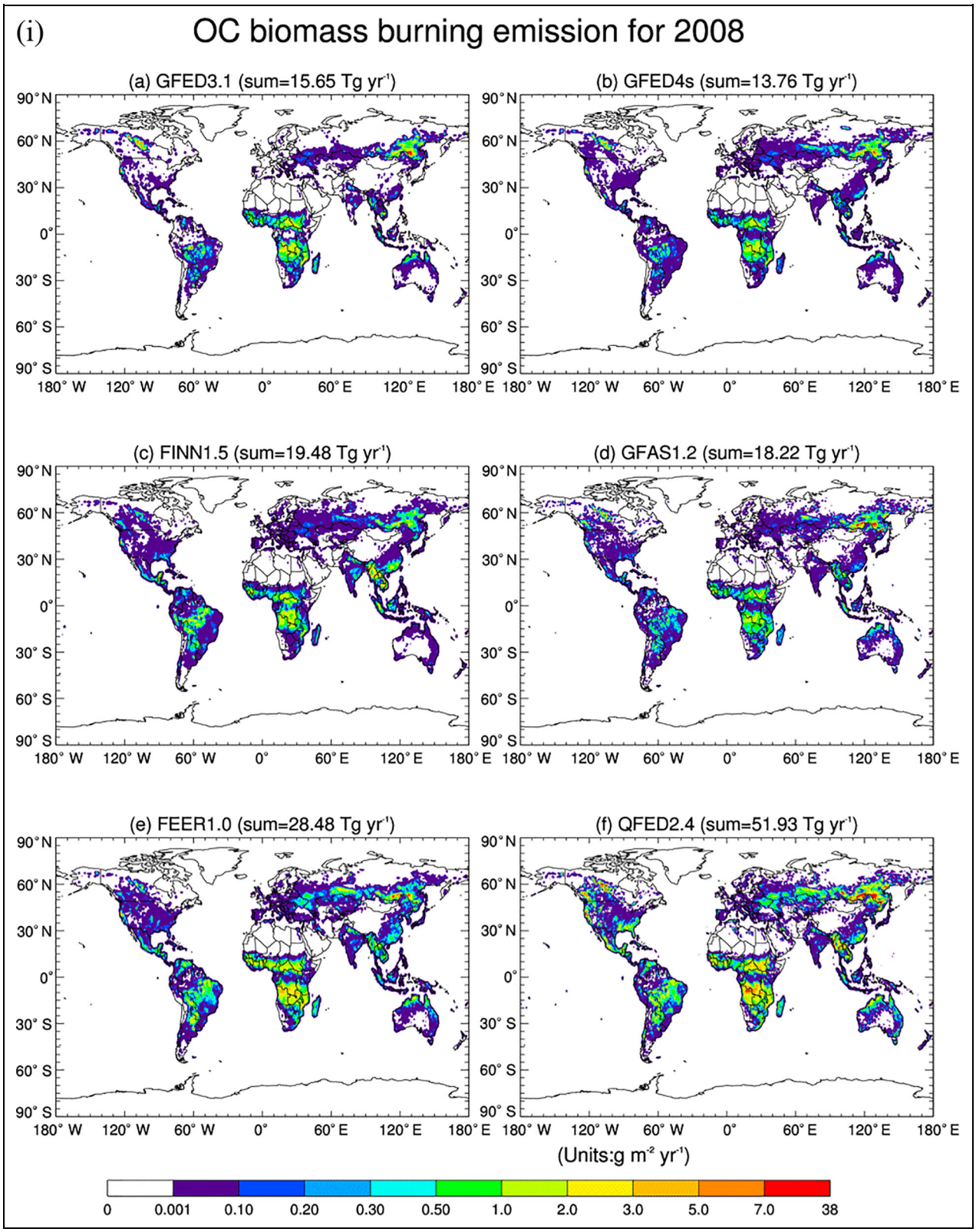

(continued).

Downloaded from http://online.ucpress.edu/elementa/article-pdf/13/1/00089/895115/elementa.2024.00089.pdf by guest on 29 September 2025

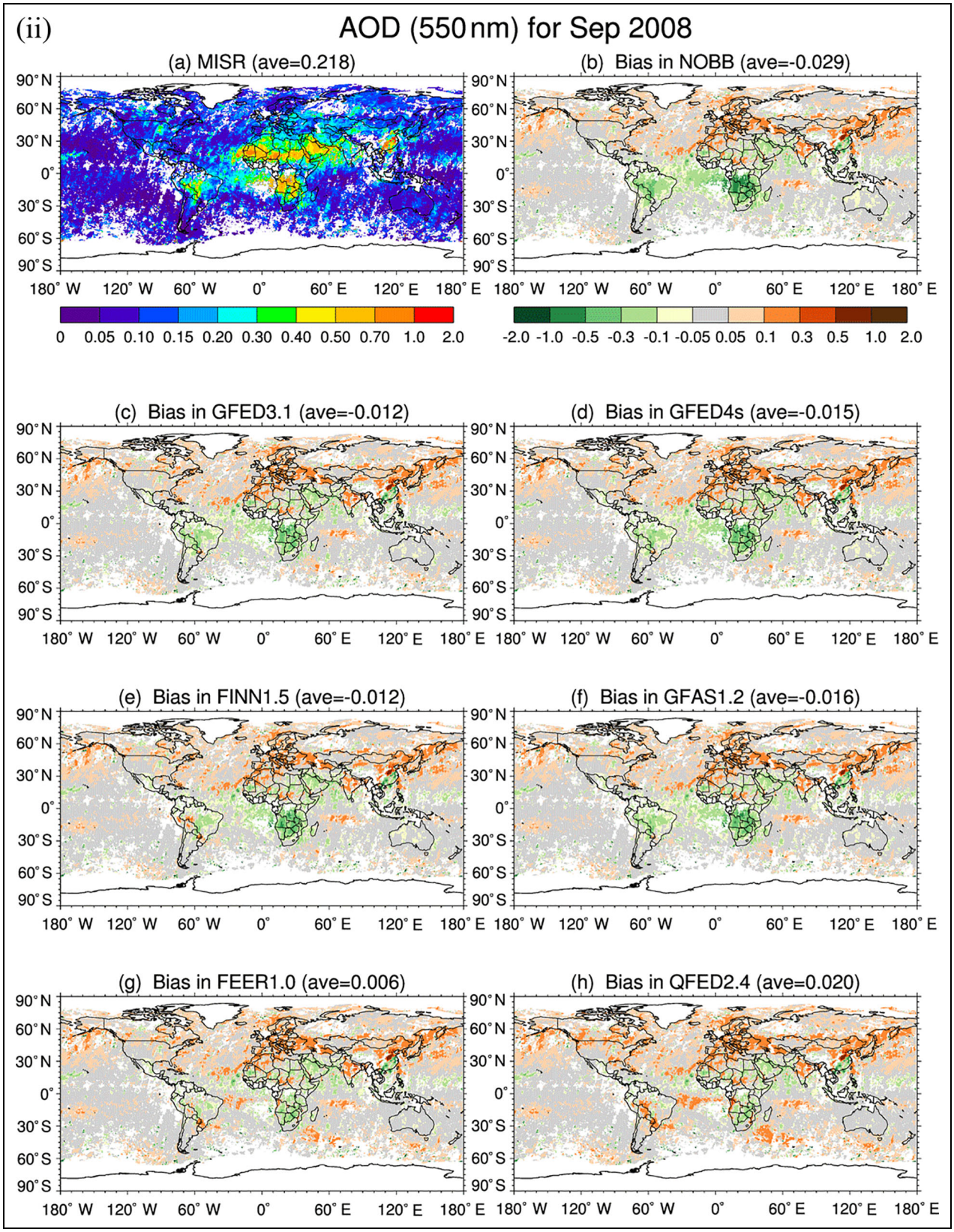

Figure 5. (i) Intercomparison of several BB OC emissions, and (ii) the resulting AOD when they are applied in a model. Figures from Pan et al. (2020).

Downloaded from http://online.ucpress.edu/elementa/article-pdf/13/1/00089/895115/elementa.2024.00089.pdf by guest on 29 September 2025

Singapore; **Figure 7**). They reported that the main challenges include accounting for the high fuel consumption in peatlands and high cloud cover and thick smoke obscuring fire disturbances, detected as either thermal anomalies or abrupt changes in surface reflectance (Giglio et al., 2016; 2018). First, some inventories do not partition peatlands into a separate land cover type, and thus do not account for differences in fuel consumption and EFs (Akagi et al., 2011; van der Werf et al., 2017; Andreae, 2019). Model simulations using inventories with peat fire specifications, such as GFASv1.2 and GFED4s, better captured the high anomalies in smoke concentrations observed at ground monitors in Singapore and Malaysia in high fire years such as 2006 and 2015 compared to other inventories (**Figure 7**). Second, as seen in 2015, thick haze during severe fire seasons can hinder fire detection even further, leading to underestimates in fire emissions. Model simulations using inventories that adjusted for such cloud/haze gaps such as GFASv1.2 and QFED2.5r1 see higher temporal correlations with smoke concentrations observed at ground monitors.

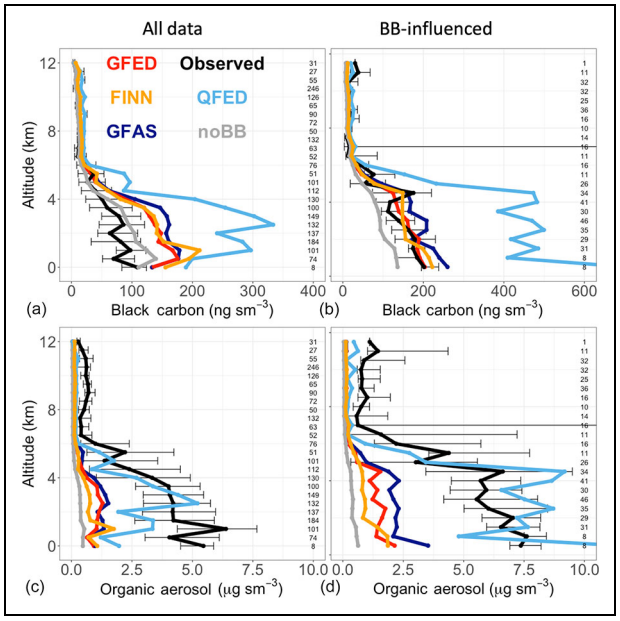

Figure 6. Intercomparison of BC (a, b) and organic aerosol (c, d) vertical profiles from a model using several BB emissions compared to aircraft-based measurements in North America. Figure from Carter et al. (2020).

Desservettaz et al. (2022) carried out a focused intercomparison study of Australian BB CO emissions estimates from FINNv1.5, GFED4s, and QFEDv2.4, processed through chemical transport models. FINNv1.5 significantly underestimated emissions from savanna fires in northern Australia when compared to GFED4s and QFEDv2.4—an order of magnitude lower than the latter. This discrepancy was so pronounced that models driven by FINNv1.5 could not replicate the observed levels and patterns of CO in the region. Wiedinmyer et al. (2023) note that the updated FINNv2.5 has increased CO emissions for the region, but remains lower than GFAS, QFED, and FEER. GFED4s and QFEDv2.4 inventories showed much closer agreement in their estimates for Australian emissions. However, QFEDv2.4 provided consistently higher emission estimates in Australia overall.

Regionally, the magnitude and temporal variability of fire emissions may differ substantially among different global inventories, and the performance of inventories may differ accordingly. Importantly, efforts toward standardization of core inputs and adjustments for constructing inventories, such as land cover classes and cloud/haze gap adjustments can reduce the variation in estimates across fire inventories. Simultaneously, region-specific adjustments of inventories, such as with household survey data of agricultural fire practices (Liu et al., 2020b) or geostationary satellite observations to improve the fire diurnal cycle (Li et al., 2022), can help to inform and

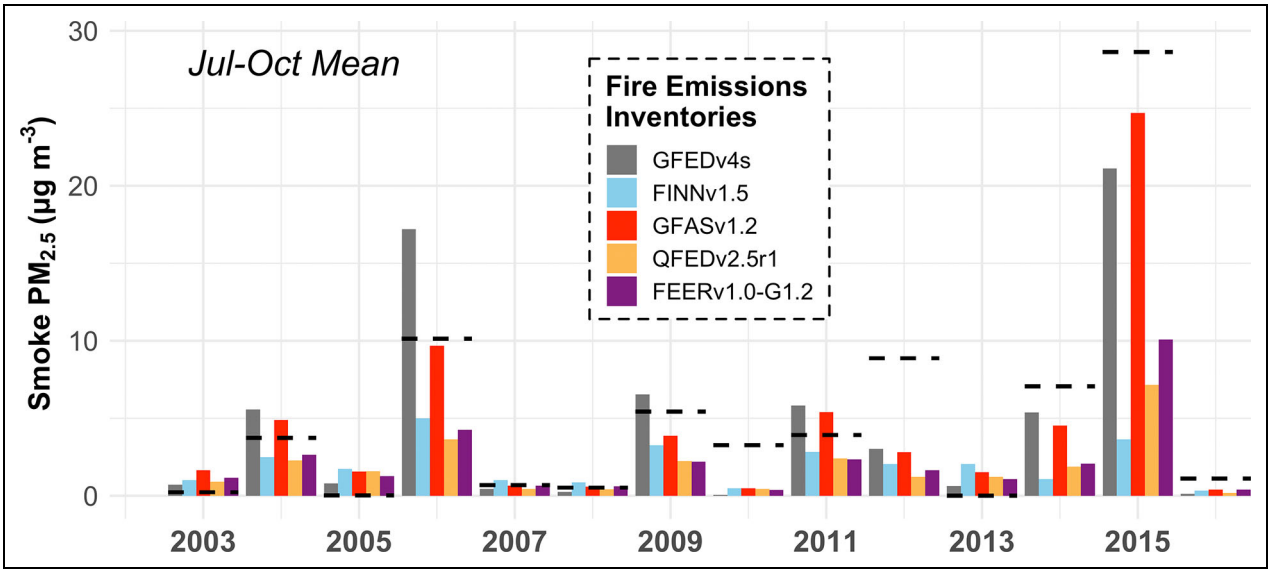

Figure 7. Intercomparison of $PM_{2.5}$ in Indonesia using several BB emissions and comparison to observed $PM_{2.5}$ (dashed lines). Figure from Liu et al. (2020a).

Downloaded from http://online.ucpress.edu/elementa/article-pdf/13/1/00089/895115/elementa.2024.00089.pdf by guest on 29 September 2025

improve global inventories. Online tools such as FIRECAM (https://globalfires.earthengine.app/view/firecam) can provide end-users with a first-order assessment of differences among global fire inventories for a study region of interest (Liu et al., 2020a).

Satellite observations of atmospheric composition related to BB smoke, in particular TROPOMI CO as used by Griffin et al. (2024), described above, have been playing a growing role in evaluating and consolidating BB emissions at regional scales. Recent studies for Australia (van der Velde et al., 2021), Southern Africa (van der Velde et al., 2024), boreal North America and Eurasia (Zheng et al., 2023), and Canada (Byrne et al., 2024) have utilized inverse modeling approaches to constrain BB emissions estimated by some, although not all, of the datasets described in Section 3, and highlight the potential of atmospheric observations for addressing uncertainties in BB emission estimation.

5. Future directions and recommendations

The FEW in November 2023 provided a timely opportunity to bring together the BB emissions community to present and discuss the state-of-the-art in BB emission estimation, comparing some of the most widely used datasets and their continued development with changes in the availability of the observations. The upcoming decommissioning of the 2 MODIS instruments marks a significant change in the global observing system and the end of a remarkable era of satellite observations for BB emissions covering the past 2 decades. Of the other sensors providing fire observations, the VIIRS instruments launched on NOAA polar-orbiting satellites are already being used in the production of some BB emissions datasets using active fire observations. VIIRS and observations from the other sensors listed in the introduction are planned for implementation in datasets to ensure provision of BB emissions estimates in the post-MODIS era.

5.1. Development, and uptake, of satellite burned area products from VIIRS and other instruments

A VIIRS burned area product has been developed but has not yet been used in the production of BB emissions. While active fire observations provide the NRT capability required for operational air quality forecasting, the BB emissions from FRP are often calibrated against BB estimates derived from burned area. Similarly, recent developments and applications of Artificial Intelligence (AI) for burned area and BB emission estimation strongly depend on training and calibration against the empirical burned area products. Therefore, continued development and availability of burned area datasets from the available sensors is strongly recommended.

5.2. Mapping of the fine scale heterogeneity in fuel type and condition

The variability of fuel type and condition, defined by biogeography, climate, and weather, is a major factor impacting emission amount, rate, and composition. Mapping the inherent heterogeneity of fuels at appropriate scales is important for accurate smoke modeling. For local to landscape-scale smoke modeling, fuel type and condition are important to map at fine scales. In contrast, global approaches apply broad assumptions about fuel type and condition but still require an understanding of the underlying heterogeneity in these factors to accurately parametrize at a larger scale and properly account for variability in combustion and emissions.

5.3. Identification of spurious signals detections and information gaps in satellite FRP products

The higher resolution of the VIIRS measurements compared to MODIS makes them more susceptible to spurious signals from non-fire thermal anomalies (such as active volcanoes, gas flaring, solar farms, and shallow coastal waters) and continued improvement in methodologies to account for these errors of commission is also recommended. Additionally, accurate and regularly updated maps of biomes and fuels, especially global peatlands where fires are difficult to detect and quantify, are recommended to help remove omission errors, which can be a large source of uncertainty in BB emission estimation. Improved accounting of small fires in GFED5, for example, highlights their significant contribution to the global total emission burden (Chen et al., 2023) and should be factored into spurious signal detection and updated biome and fuel maps.

5.4. Regional modeling studies and comparison against existing datasets

In order to best validate fire emissions datasets, atmospheric models must use those datasets to simulate the resulting atmospheric concentration of smoke-related pollutants and then compare model output to observed concentrations. However, models have other uncertainties in addition to emissions uncertainties. An important step is to characterize and quantify the uncertainties by running multiple simulations with different BB datasets in one model framework (as some studies mentioned in Section 4 have done) as well as using multiple models to run simulations with the same BB datasets. Both of these are proposed for the HTAP3 Fires model intercomparison project (Whaley et al., 2025), which started in 2025. Multiple regions and pollutant species will be targeted in this intercomparison. Also, in order to isolate the uncertainty that appears due to EFs, an experiment in which each fire emissions dataset uses the same EFs—such as those from NEIVA—would remove that source of variability.

After quantifying sources of variability in model simulations, a more precise understanding of differences can be gained when comparing model results with observations, such as those from satellites. Regional evaluation against in situ measurements, including vertically resolved aircraft campaign measurements of multiple smoke pollutants would also be valuable. The FIREX-AQ, WE-CAN, BBFLUX, BBOP, aircraft campaigns represent some of the best field observations of BB conditions and coordinated effort of model simulations against these datasets can help identify systematic biases in fire emissions input.

Downloaded from http://online.ucpress.edu/elementa/article-pdf/13/1/00089/895115/elementa.2024.00089.pdf by guest on 29 September 2025

5.5. Representation of the diurnal cycle and plume rise in BB emissions

Finally, we know that the diurnal cycle in fire emissions is important, and difficult to represent when so much dependence is on once-or-twice-daily satellite observations. However, it is well known that fire emissions vary greatly over the day and night and thus, for many model applications, this needs to be well represented. In addition, injection height and vertical distribution of smoke plumes into the atmosphere (e.g., Feng et al., 2024) is also very important as it determines where the fire emissions are added to the atmosphere, which further impacts the transport, chemistry, and lifetime of fire emitted trace gases and aerosols. More studies are needed to address injection height of fire plumes, and indeed, the HTAP3 Fires study will also include injection height perturbation experiments (Whaley et al., 2025). The injection height of fire plumes and diurnal cycle of fire emissions are also a coupled problem due to the diurnal cycle of meteorology (Tang et al., 2022). For example, during the day, when fire emissions tend to be stronger, vertical mixing and convection are also more intense. At night, both fire emissions and vertical mixing tend to weaken. Incorporating both injection height and the diurnal cycle of fire emissions in the model could have a synergistic effect, amplifying their combined impact.

5.6. The evolving research landscape and final remarks

In the time that has elapsed since the FEW in November 2023 several new studies have been published which highlight advances in modeling, and the potential application of AI and machine learning (ML), to address key uncertainties in some of the inputs to BB emission estimation. For example, McNorton and Di Giuseppe (2024) developed the combined use of satellite observations of above ground fuel and modeled Net Ecosystem Exchange to improve fuel characteristics including live and dead fuel moisture. Similarly, Forkel et al. (2025) applied satellite observations and ML to address uncertainties in dry matter burned by biome and fire type, taking into account land-use change/drought and dynamic EFs, with the further application of satellite observations of atmospheric constituents to constrain estimated emissions. These studies, along with the satellite inverse modeling studies cited earlier, further highlight the critical importance of satellite observations for BB emission estimation from different biomes and fuel availability, and the potential for isolating some of the key uncertainties at regional and global scales.

Imminent changes to the available observations, and continuing advances under the rapidly developing discipline of wildfire science, make it imperative to identify and better quantify the key uncertainties in BB emissions. The outcomes and recommendations presented in this manuscript, and the goals of the IGAC BBURNED activity, represent the forward-looking multidisciplinary approach required to pool resources for improving BB emission estimation and its uncertainties.

Data accessibility statement

All data that were considered in this work are available in the cited literature.

Supplemental files

The supplemental files for this article can be found as follows:

Supplementary Information.pdf

Acknowledgments

We would like to start by thanking Amber Soja, an anonymous reviewer and the editors for their constructive comments and suggestions in reviewing the manuscript. We thank NSF NCAR for hosting the virtual Fire Emission Workshop (FEW), and especially UCAR Multimedia Technician Joseph Ehrman for providing technical help before, during, and after the workshop, and Software Engineer Carl Drews for help with posting workshop recordings. We also thank NSF NCAR/ACOM for hosting the recordings on their YouTube site. NSF NCAR/ACOM also provides website hosting for BBURNED and FEW. Finally, we express thanks to the Scientific Steering Committee of HTAP (Tim Butler, Terry Keating, Jacek Kaminsky, and Rosa Wu) for their contributions to planning and running the workshop. The BBURNED activity is supported by IGAC and overseen by IGAC steering committee member Louisa Emmons.

Funding

The Copernicus Atmosphere Monitoring Service is operated by the European Centre for Medium-Range Weather Forecasts (ECMWF) on behalf of the European Commission as part of the Copernicus Programme (http://copernicus.eu). The participation of Clare Paton-Walsh (Murphy) and Maximilien Desservettaz was supported by the New South Wales Department of Climate Change, Energy, the Environment and Water, within the Bushfire and Natural Hazards Research Centre via the project known as RUSH (Research for Understanding Smoke Hazards). Edward Hyer's participation was supported by the Office of Naval Research Code 32. Nancy French's participation was supported with internal funding from Michigan Tech Research Institute and NASA Interdisciplinary Science Program Grant #80NSSC24K0299. Contribution of Mikhail Sofiev was funded by a project of Finnish Research Council VFSP-WASE (grant 359421), Andreas Uppstu was supported by EU Horizon project FirEUrisk (grant number 101003890), and Julia Palamarchuk was funded by a Finnish Research Council project HEATCOST (grant 334798).

Competing interests

The authors have declared that no competing interests exist.

Disclaimer

Views expressed in this paper are those of author(s) and do not necessarily reflect those of NOAA or the Department of Commerce.

Downloaded from http://online.ucpress.edu/elementa/article-pdf/13/1/00089/895115/elementa.2024.00089.pdf by guest on 29 September 2025

Author contributions

Contributed to conception and design: MP, CHW, NHFF, RRB.
Contributed to analysis and interpretation of data: All authors.
Drafted and/or revised the article: All authors.
Approved the submitted version for publication: All authors.

References

Akagi, SK, **Yokelson, RJ**, **Wiedinmyer, C**, **Alvarado, MJ**, **Reid, JS**, **Karl, T**, **Crounse, JD**, **Wennberg, PO.** 2011. Emission factors for open and domestic biomass burning for use in atmospheric models. *Atmospheric Chemistry and Physics* **11**: 4039–4072. DOI: https://doi.org/10.5194/acp-11-4039-2011.

Andela, N, **Kaiser, JW**, **van der Werf, GR**, **Wooster, MJ.** 2015. New fire diurnal cycle characterizations to improve fire radiative energy assessments made from MODIS observations. *Atmospheric Chemistry and Physics* **15**: 8831–8846. DOI: https://doi.org/10.5194/acp-15-8831-2015.

Anderson, K, **Chen, J**, **Englefield, P**, **Griffin, D**, **Makar, PA**, **Thompson, D.** 2024. The Global Forest Fire Emissions Prediction System version 1.0. *Geoscientific Model Development* **17**: 7713–7749. DOI: https://doi.org/10.5194/gmd-17-7713-2024.

Andreae, MO. 2019. Emission of trace gases and aerosols from biomass burning—An updated assessment. *Atmospheric Chemistry and Physics* **19**: 8523–8546. DOI: https://doi.org/10.5194/acp-19-8523-2019.

Andreae, MO, **Merlet, P.** 2001. Emission of trace gases and aerosols from biomass burning. *Global Biogeochemical Cycles* **15**(4): 955–966. DOI: https://doi.org/10.1029/2000GB001382.

Balch, JK, **Abatzoglou, JT**, **Joseph, MB**, **Koontz, MJ**, **Mahood, AL**, **McGlinchy, J**, **Cattau, ME**, **Williams, AP.** 2022. Warming weakens the night-time barrier to global fire. *Nature* **602**: 442–448. DOI: https://doi.org/10.1038/s41586-021-04325-1.

Binte Shahid, S, **Lacey, FG**, **Wiedinmyer, C**, **Yokelson, RJ**, **Barsanti, KC.** 2024. NEIVAv1.0: Next-generation Emissions InVentory expansion of Akagi et al. (2011) version 1.0. *Geoscientific Model Development* **17**: 7679–7711. DOI: https://doi.org/10.5194/gmd-17-7679-2024.

Bowman, DMJS, **Kolden, CA**, **Abatzoglou, JT**, **Johnston, FH**, **van der Werf, GR**, **Flannigan, M.** 2020. Vegetation fires in the Anthropocene. *Natural Reviews Earth and Environment* **1**: 500–515. DOI: https://doi.org/10.1038/s43017-020-0085-3.

Bright, BC, **Hudak, AT**, **McCarley, TR**, **Spannuth, A**, **Sánchez-López, N**, **Ottmar, RD**, **Soja, AJ.** 2022. Multitemporal lidar captures heterogeneity in fuel loads and consumption on the Kaibab Plateau. *Fire Ecology* **18**(1): 18. DOI: https://doi.org/10.1186/s42408-022-00142-7.

Byrne, B, **Liu, J**, **Bowman, KW**, **Pascolini-Campbell, M**, **Chatterjee, A**, **Pandey, S**, **Miyazaki, K**, **van der Werf, GR**, **Wunch, D**, **Wennberg, PO**, **Roehl, CM**, **Sinha, S.** 2024. Carbon emissions from the 2023 Canadian wildfires. *Nature* **633**: 835–839. DOI: https://doi.org/10.1038/s41586-024-07878-z.

Carter, TS, **Heald, CL**, **Jimenez, JL**, **Campuzano-Jost, P**, **Kondo, Y**, **Moteki, N**, **Schwarz, JP**, **Wiedinmyer, C**, **Darmenov, AS**, **da Silva, AM**, **Kaiser, JW.** 2020. How emissions uncertainty influences the distribution and radiative impacts of smoke from fires in North America. *Atmospheric Chemistry and Physics* **20**: 2073–2097. DOI: https://doi.org/10.5194/acp-20-2073-2020.

Caseiro, A, **Gehrke, B**, **Rucker, G**, **Leimbach, D**, **Kaiser, JW.** 2020. Gas flaring activity and black carbon emissions in 2017 derived from the Sentinel-3A Sea and Land Surface Temperature Radiometer. *Earth System Science Data* **12**: 2137–2155. DOI: https://doi.org/10.5194/essd-12-2137-2020.

Chen, Y, **Hall, J**, **van Wees, D**, **Andela, N**, **Hantson, S**, **Giglio, L**, **van der Werf, GR**, **Morton, DC**, **Randerson, JT.** 2023. Multi-decadal trends and variability in burned area from the fifth version of the Global Fire Emissions Database (GFED5). *Earth System Science Data* **15**: 5227–5259. DOI: https://doi.org/10.5194/essd-15-5227-2023.

Chowdhury, S, **Hänninen, R**, **Sofiev, M**, **Aunan, K.** 2024. Fires as a source of annual ambient $PM_{2.5}$ exposure and chronic health impacts in Europe. *Science of The Total Environment* **922**: 171314. DOI: https://doi.org/10.1016/j.scitotenv.2024.171314.

Christian, TJ, **Kleiss, B**, **Yokelson, RJ**, **Holzinger, R**, **Crutzen, PJ**, **Hao, WM**, **Saharjo, BH**, **Ward, DE.** 2003. Comprehensive laboratory measurements of biomass-burning emissions: 1. Emissions from Indonesian, African, and other fuels. *Journal of Geophysical Research: Atmospheres* **108**(23). DOI: https://doi.org/10.1029/2003jd003704.

Cova, GR, **Prichard, SJ**, **Rowell, E**, **Drye, B**, **Eagle, P**, **Kennedy, MC**, **Nemens, DG.** 2023. Evaluating close-range photogrammetry for 3D understory fuel characterization and biomass prediction in pine forests. *Remote Sensing* **15**(19): 4837. DOI: https://doi.org/10.3390/rs15194837.

Csiszar, I, **Schroeder, W**, **Giglio, L**, **Ellicott, E**, **Vadrevu, KP**, **Justice, CO**, **Wind, B.** 2014. Active fires from the Suomi NPP Visible Infrared Imaging Radiometer Suite: Product status and first evaluation results. *Journal of Geophysical Research: Atmospheres* **119**(2): 803–816. DOI: https://doi.org/10.1002/2013JD020453.

Curto, A, **Nunes, J**, **Milà, C**, **Nhacolo, A**, **Hänninen, R**, **Sofiev, M**, **Valentín, A**, **Saúte, F**, **Kogevinas, M**, **Sacoor, C**, **Bassat, Q**, **Tonne, C.** 2024. Associations between landscape fires and child morbidity in southern Mozambique: A time-series study. *The Lancet Planetary Health* **8**: e41–e50. DOI: https://doi.org/10.1016/S2542-5196(23)00251-6.

Darmenov, AS, **da Silva, A.** 2015. The Quick Fire Emissions Dataset (QFED): Documentation of versions 2.1, 2.2 and 2.4. NASA/TM-2015-104606/, vol. 38.

Downloaded from http://online.ucpress.edu/elementa/article-pdf/13/1/00089/895115/elementa.2024.00089.pdf by guest on 29 September 2025

Available at https://gmao.gsfc.nasa.gov/media/publications/zbly36ziNFDFbmYmvhQeVqPhUo/Darmenov796.pdf.

Desservettaz, MJ, **Fisher, JA**, **Luhar, AK**, **Woodhouse, MT**, **Bukosa, B**, **Buchholz, RR**, **Wiedinmyer, C**, **Griffith, DWT**, **Krummel, PB**, **Jones, NB**, **Deutscher, NM**, **Greenslade, GW.** 2022. Australian fire emissions of carbon monoxide estimated by global biomass burning inventories: Variability and observational constraints. *Journal of Geophysical Research: Atmospheres* **127**: e2021JD035925. DOI: https://doi.org/10.1029/2021JD035925.

Eva, H, **Lambin, EF.** 1998. Burnt area mapping in Central Africa using ATSR data. *International Journal of Remote Sensing* **19**(18): 3473–3497. DOI: https://doi.org/10.1080/014311698213768.

Feng, X, **Mickley, LJ**, **Bell, ML**, **Liu, T**, **Fisher, JA**, **Val Martin, M.** 2024. Improved estimates of smoke exposure during Australia fire seasons: Importance of quantifying plume injection heights. *Atmospheric Chemistry and Physics* **24**: 2985–3007. DOI: https://doi.org/10.5194/acp-24-2985-2024.

Fisher, JA, **Jacob, DJ**, **Purdy, MT**, **Kopacz, M**, **Le Sager, P**, **Carouge, C**, **Holmes, CD**, **Yantosca, RM**, **Batchelor, RL**, **Strong, K**, **Diskin, GS**, **Fuelberg, HE**, **Holloway, JS**, **Hyer, EJ**, **McMillan, WW**, **Warner, J**, **Streets, DG**, **Zhang, Q**, **Wang, Y**, **Wu, S.** 2010. Source attribution and interannual variability of Arctic pollution in spring constrained by aircraft (ARCTAS, ARCPAC) and satellite (AIRS) observations of carbon monoxide. *Atmospheric Chemistry and Physics* **10**: 977–996. DOI: https://doi.org/10.5194/acp-10-977-2010.

Forkel, M, **Wessollek, C**, **Huijnen, V**, **Andela, N**, **de Laat, A**, **Kinalczyk, D**, **Marrs, C**, **van Wees, D**, **Bastos, A**, **Ciais, P**, **Fawcett, D**, **Kaiser, JW**, **Klauberg, C**, **Kutchartt, E**, **Leite, R**, **Li, W**, **Silva, C**, **Sitch, S**, **Goncalves De Souza, J**, **Zaehle, S**, **Plummer, S.** 2025. Burning of woody debris dominates fire emissions in the Amazon and Cerrado. *Nature Geoscience* **18**: 140–147. DOI: https://doi.org/10.1038/s41561-024-01637-5.

Freitas, SR, **Longo, KM**, **Trentmann, J**, **Latham, D.** 2010. Technical Note: Sensitivity of 1-D smoke plume rise models to the inclusion of environmental wind drag. *Atmospheric Chemistry and Physics* **10**: 585. DOI: https://doi.org/10.5194/acp-10-585-2010.

French, NHF, **Goovaerts, P**, **Kasischke, ES.** 2004. Uncertainty in estimating carbon emissions from boreal forest fires. *Journal of Geophysical Research: Atmospheres* **109**: D14S08. DOI: https://doi.org/10.1029/2003JD003635.

French, NHF, **Hudak, AT.** 2024. Biomass burning fuel consumption and emissions for air quality, in Loboda, TV, French, NHF, Puett RC eds., *Landscape fire, smoke, and health: Linking biomass burning emissions to human well-being*. Hoboken, NJ: John Wiley & Sons, Inc. (Geophysical Monograph, vol. 280). DOI: https://doi.org/10.1002/9781119757030.

French, NHF, **Prichard, SJ**, **Billimire, MG**, **Kennedy, M**, **Andreu, AG**, **Eagle, PC**, **Tanzer, D**, **McKenzie, D**, **Ottmar, R.** 2020. North American Wildland Fuels Database. Available at https://fuels.mtri.org/. Accessed April 14, 2025.

Giglio, L, **Boschetti, L**, **Roy, DP**, **Humber, ML**, **Justice, CO.** 2018. The Collection 6 MODIS burned area mapping algorithm and product. *Remote Sensing of Environment* **217**: 72–85. DOI: https://doi.org/10.1016/j.rse.2018.08.005.

Giglio, L, **Hall, JV**, **Humber, M**, **Argueta, F**, **Boschetti, L**, **Roy, D.** 2024a. Collection 2 VIIRS Burned Area Product User's Guide Version 1.1. NASA EOSDIS Land Processes Distributed Active Archive Center. DOI: https://doi.org/10.5067/VIIRS/VNP64A1.002. Accessed March 18, 2025.

Giglio, L, **Kendall, JD**, **Tucker, CJ.** 2000. Remote sensing of fires with the TRMM VIRS. *International Journal of Remote Sensing* **21**(1): 203–207. DOI: https://doi.org/10.1080/014311600211109.

Giglio, L, **Randerson, JT**, **van der Werf, GR.** 2013. Analysis of daily, monthly, and annual burned area using the fourth-generation global fire emissions database (GFED4). *Journal of Geophysical Research: Biogeosciences* **118**: 317–328. DOI: https://doi.org/10.1002/jgrg.20042.

Giglio, L, **Roy, DP**, **Humber, ML**, **Ellicott, E**, **Zubkova, M**, **Justice, CO.** 2024b. Mapping and characterizing fire, in Loboda, TV, French, NHF, Puett, RC eds., *Landscape fire, smoke, and health: Linking biomass burning emissions to human well-being*. Hoboken, NJ: John Wiley & Sons, Inc. (Geophysical Monograph, vol. 280). DOI: https://doi.org/10.1002/9781119757030.

Giglio, L, **Schroeder, W**, **Justice, CO.** 2016. The collection 6 MODIS active fire detection algorithm and fire products. *Remote Sensing of Environment* **178**: 31–41. DOI: https://doi.org/10.1016/j.rse.2016.02.054.

Griffin, D, **Chen, J**, **Anderson, K**, **Makar, P**, **McLinden, CA**, **Dammers, E**, **Fogal, A.** 2024. Biomass burning CO emissions: Exploring insights through TROPOMI-derived emissions and emission coefficients. *Atmospheric Chemistry and Physics* **24**: 10159–10186. DOI: https://doi.org/10.5194/acp-24-10159-2024.

Hänninen, R, **Sofiev, M**, **Uppstu, A**, **Kouznetsov, R.** 2024. Daily surface concentration of fire related PM2.5 for 2003–2023, modelled by SILAM CTM when using the MODIS satellite data for the fire radiative power [dataset]. Finnish Meteorological Institute. DOI: https://doi.org/10.57707/FMI-B2SHARE.D1CAC971B3224D438D5304E945E9F16C.

Heald, CL, **Jacob, DJ**, **Palmer, PI**, **Evans, MJ**, **Sachse, GW**, **Singh, HB**, **Blake, DR.** 2003. Biomass burning emission inventory with daily resolution: Application to aircraft observations of Asian outflow. *Journal of Geophysical Research: Atmospheres* **108**(D21): 8811. DOI: https://doi.org/10.1029/2002JD003082.

Hope, ES, **McKenney, DW**, **Johnston, LM**, **Johnston, JM.** 2024. A cost-benefit analysis of WildFireSat,

Downloaded from http://online.ucpress.edu/elementa/article-pdf/13/1/00089/895115/elementa.2024.00089.pdf by guest on 29 September 2025

a wildfire monitoring satellite mission for Canada. *PLoS ONE* **19**(5): e0302699. DOI: https://doi.org/10.1371/journal.pone.0302699.

Hyer, EJ, **Chew, BN.** 2010. Aerosol transport model evaluation of an extreme smoke episode in Southeast Asia. *Atmospheric Environment* **44**(11): 1422–1427. DOI: https://doi.org/10.1016/j.atmosenv.2010.01.043.

Ichoku, C, **Ellison, L.** 2014. Global top-down smoke-aerosol emissions estimation using satellite fire radiative power measurements. *Atmospheric Chemistry and Physics* **14**: 6643–6667. DOI: https://doi.org/10.5194/acp-14-6643-2014.

Ichoku, C, **Kaufman, YJ.** 2005. A method to derive smoke emission rates from MODIS fire radiative energy measurements. *IEEE Transactions on Geoscience and Remote Sensing* **43**(11): 2636–2649. DOI: https://doi.org/10.1109/TGRS.2005.857328.

Ichoku, C, **Martins, JV**, **Kaufman, YJ**, **Wooster, MJ**, **Freeborn, PH**, **Hao, WM**, **Baker, S**, **Ryan, CA**, **Nordgren, BL.** 2008. Laboratory investigation of fire radiative energy and smoke aerosol emissions. *Journal of Geophysical Research: Atmospheres* **113**: D14S09. DOI: https://doi.org/10.1029/2007JD009659.

Jones, MW, **Veraverbeke, S**, **Andela, N**, **Doerr, SH**, **Kolden, C**, **Mataveli, G**, **Lucrecia Pettinari, M**, **Le Quéré, C**, **Rosan, TM**, **van der Werf, GR**, **Wees, D**, **Abatzoglou, JT.** 2024. Global rise in forest fire emissions linked to climate change in the extratropics. *Science* **386**(6719). DOI: https://doi.org/10.1126/science.adl5889.

Kaiser, JW, **Heil, A**, **Andreae, MO**, **Benedetti, A**, **Chubarova, N**, **Jones, L**, **Morcrette, JJ**, **Razinger, M**, **Schultz, MG**, **Suttie, M**, **van der Werf, GR.** 2012. Biomass burning emissions estimated with a global fire assimilation system based on observed fire radiative power. *Biogeosciences* **9**(1). DOI: https://doi.org/10.5194/bg-9-527-2012.

Kaiser, JW, **Suttie, M**, **Flemming, J**, **Morcrette, JJ**, **Boucher, O**, **Schultz, MG.** 2009. Global real-time fire emission estimates based on space-borne fire radiative power observations. *AIP Conference Proceedings* **1100**: 645–648. DOI: https://doi.org/10.1063/1.3117069.

Kennedy, MC, **Prichard, SJ**, **McKenzie, D**, **French, NHF.** 2020. Quantifying how sources of uncertainty in combustible biomass propagate to prediction of wildland fire emissions. *International Journal of Wildland Fire* **29**(9): 793–806. DOI: https://doi.org/10.1071/WF19160.

Larkin, NK, **Strand, TM**, **Drury, SA**, **Raffuse, SM**, **Solomon, RC**, **O'Neill, SM**, **Wheeler, N**, **Huang, S**, **Roring, M**, **Hafner, HR.** 2012. Phase 1 of the Smoke and Emissions Model Intercomparison Project (SEMIP): Creation of SEMIP and evaluation of current models. Final Report to the Joint Fire Science Program Project #08-1-6-10. Available at https://digitalcommons.unl.edu/jfspresearch/42/. Accessed July 12, 2024.

Li, F, **Zhang, X**, **Kondragunta, S.** 2021. Highly anomalous fire emissions from the 2019–2020 Australian bushfires. *Environmental Research Communications* **3**: 105005. DOI: https://doi.org/10.1088/2515-7620/ac2e6f.

Li, F, **Zhang, X**, **Kondragunta, S**, **Lu, X**, **Csiszar, I**, **Schmidt, CC.** 2022. Hourly biomass burning emissions product from blended geostationary and polar-orbiting satellites for air quality forecasting applications. *Remote Sensing of Environment* **281**: 113237. DOI: https://doi.org/10.1016/j.rse.2022.113237.

Liu, T, **Mickley, LJ**, **Marlier, ME**, **DeFries, RS**, **Khan, MF**, **Latif, MT**, **Karambelas, A.** 2020a. Diagnosing spatial biases and uncertainties in global fire emissions inventories: Indonesia as regional case study. *Remote Sensing of Environment* **237**: 111517. DOI: https://doi.org/10.1016/j.rse.2019.111557.

Liu, T, **Mickley, LJ**, **Singh, S**, **Jain, M**, **DeFries, RS**, **Marlier, ME.** 2020b. Crop residue burning practices across north India inferred from household survey data: Bridging gaps in satellite observations. *Atmospheric Environment: X* **8**: 100091. DOI: https://doi.org/10.1016/j.aeaoa.2020.100091.

Lynch, P, **Reid, JS**, **Westphal, DL**, **Zhang, J**, **Hogan, TF**, **Hyer, EJ**, **Curtis, CA**, **Hegg, DA**, **Shi, Y**, **Campbell, JR**, **Rubin, JI**, **Sessions, WR**, **Turk, FJ**, **Walker, AL.** 2016. An 11-year global gridded aerosol optical thickness reanalysis (v1.0) for atmospheric and climate sciences. *Geoscientific Model Development* **9**: 1489–1522. DOI: https://doi.org/10.5194/gmd-9-1489-2016.

McNorton, JR, **Di Giuseppe, F.** 2024. A global fuel characteristic model and dataset for wildfire prediction. *Biogeosciences* **21**: 279–300. DOI: https://doi.org/10.5194/bg-21-279-2024.

Mota, B, **Wooster, MJ.** 2018. A new top-down approach for directly estimating biomass burning emissions and fuel consumption rates and totals from geostationary satellite fire radiative power (FRP). *Remote Sensing of Environment* **206**: 45–62. DOI: https://doi.org/10.1016/j.rse.2017.12.016.

Mu, M, **Randerson, JT**, **van der Werf, GR**, **Giglio, L**, **Kasibhatla, P**, **Morton, D**, **Collatz, GJ**, **DeFries, RS**, **Hyer, EJ**, **Prins, EM**, **Griffith, DWT**, **Wunch, D**, **Toon, GC**, **Sherlock, V**, **Wennberg, PO.** 2011. Daily and 3-hourly variability in global fire emissions and consequences for atmospheric model predictions of carbon monoxide. *Journal of Geophysical Research: Atmospheres* **116**: D24303. DOI: https://doi.org/10.1029/2011JD016245.

Nguyen, HM, **He, J**, **Wooster, MJ.** 2023. Biomass burning CO, PM and fuel consumption per unit burned area estimates derived across Africa using geostationary SEVIRI fire radiative power and Sentinel-5P CO data. *Atmospheric Chemistry and Physics* **23**: 2089–2118. DOI: https://doi.org/10.5194/acp-23-2089-2023.

Ottmar, RD. 2014. Wildland fire emissions, carbon, and climate: Modeling fuel consumption. *Forest Ecology*

Downloaded from http://online.ucpress.edu/elementa/article-pdf/13/1/00089/895115/elementa.2024.00089.pdf by guest on 29 September 2025

and Management **317**: 41–50. DOI: https://doi.org/10.1016/j.foreco.2013.06.010.

Pan, X, **Ichoku, C**, **Chin, M**, **Bian, H**, **Darmenov, A**, **Colarco, P**, **Ellison, L**, **Kucsera, T**, **da Silva, A**, **Wang, J**, **Oda, T**, **Cui, G.** 2020. Six global biomass burning emission datasets: Intercomparison and application in one global aerosol model. *Atmospheric Chemistry and Physics* **20**: 969–994. DOI: https://doi.org/10.5194/acp-20-969-2020.

Peterson, D, **Hyer, E**, **Wang, J.** 2013. A short-term predictor of satellite-observed fire activity in the North American boreal forest: Toward improving the prediction of smoke emissions. *Atmospheric Environment* **71**: 304–310. DOI: https://doi.org/10.1016/j.atmosenv.2013.01.052.

Prichard, SJ, **Kennedy, MC**, **Andreu, AG**, **Eagle, P**, **French, NHF.** 2019. Next-generation biomass mapping for regional emissions and carbon inventories: Incorporating uncertainty in wildland fuel characterization. *Journal of Geophysical Research: Biogeosciences* **124**. DOI: https://doi.org/10.1029/2019JG005083.

Prichard, SJ, **O'Neill, SM**, **Eagle, P**, **Andreu, AG**, **Drye, B**, **Dubowy, J**, **Urbanski, S**, **Strand, TM.** 2020. Wildland fire emission factors in North America: Synthesis of existing data, measurement needs and management applications. *International Journal of Wildland Fire* **29**(2): 132–147. DOI: https://doi.org/10.1071/WF19066.

Prichard, SJ, **Rowell, E**, **Keane, RE**, **Hudak, AT**, **Lutes, D**, **Loudermilk, EL.** 2024. Wildland fuel characterization across space and time, in Loboda, TV, French, NHF, Puett, RC eds., *Landscape fire, smoke, and health: Linking biomass burning emissions to human well-being*. Hoboken, NJ: John Wiley & Sons, Inc. DOI: https://doi.org/10.1002/9781119757030.

Prins, EM, **Menzel, WP.** 1994. Trends in South-American biomass burning detected with the GOES visible infrared spin scan radiometer atmospheric sounder from 1983 to 1991. *Journal of Geophysical Research: Atmospheres* **99**(D8): 16719–16735. DOI: https://doi.org/10.1029/94JD01208.

Randerson, JT, **Chen, Y**, **van derWerf, GR**, **Rogers, BM**, **Morton, DC.** 2012. Global burned area and biomass burning emissions from small fires. *Journal of Geophysical Research: Biogeosciences* **117**: G04012. DOI: https://doi.org/10.1029/2012JG002128.

Reid, JS, **Eck, TF**, **Christopher, SA**, **Koppmann, R**, **Dubovik, O**, **Eleuterio, DP**, **Holben, BN**, **Reid, EA**, **Zhang, J.** 2005a. A review of biomass burning emissions part III: Intensive optical properties of biomass burning particles. *Atmospheric Chemistry and Physics* **5**: 827–849. DOI: https://doi.org/10.5194/acp-5-827-2005.

Reid, JS, **Hyer, EJ**, **Prins, EM**, **Westphal, DL**, **Zhang, J**, **Wang, J**, **Christopher, SA**, **Curtis, CA**, **Schmidt, CC**, **Eleuterio, DP**, **Richardson, KA**, **Hoffman, JP.** 2009. Global monitoring and forecasting of biomass-burning smoke: Description of and lessons from the Fire Locating and Modeling of Burning Emissions (FLAMBE) Program. *IEEE Journal of Selected Topics in Applied Earth Observations and Remote Sensing* **2**(3): 144–162. DOI: https://doi.org/10.1109/JSTARS.2009.2027443.

Reid, JS, **Koppmann, R**, **Eck, TF**, **Eleuterio, DP.** 2005b. A review of biomass burning emissions part II: Intensive physical properties of biomass burning particles. *Atmospheric Chemistry and Physics* **5**: 799–825. DOI: https://doi.org/10.5194/acp-5-799-2005.

Reid, JS, **Prins, EM**, **Westphal, DL**, **Schmidt, CC**, **Richardson, KA**, **Christopher, SA**, **Eck, TF**, **Reid, EA**, **Curtis, CA**, **Hoffman, JP.** 2004. Real-time monitoring of South American smoke particle emissions and transport using a coupled remote sensing/box-model approach. *Geophysical Research Letters* **31**(6). DOI: https://doi.org/10.1029/2003GL018845.

Roberts, G, **Wooster, MJ**, **Xu, W**, **Freeborn, PH**, **Morcrette, JJ**, **Jones, L**, **Benedetti, A**, **Jiangping, H**, **Fisher, D**, **Kaiser, JW.** 2015. LSA SAF Meteosat FRP products—Part 2: Evaluation and demonstration for use in the Copernicus Atmosphere Monitoring Service (CAMS). *Atmospheric Chemistry and Physics* **15**(22): 13241–13267. DOI: https://doi.org/10.5194/acp-15-13241-2015.

Romanello, M, **Napoli, CD**, **Green, C**, **Kennard, H**, **Lampard, P**, **Scamman, D**, **Walawender, M**, **Ali, Z**, **Ameli, N**, **Ayeb-Karlsson, S**, **Beggs, PJ**, **Belesova, K**, **Berrang Ford, L**, **Bowen, K**, **Cai, W**, **Callaghan, M**, **Campbell-Lendrum, D**, **Chambers, J**, **Cross, TJ**, **Van Daalen, KR**, **Dalin, C**, **Dasandi, N**, **Dasgupta, S**, **Davies, M**, **Dominguez-Salas, P**, **Dubrow, R**, **Ebi, KL**, **Eckelman, M**, **Ekins, P**, **Freyberg, C**, **Gasparyan, O**, **Gordon-Strachan, G**, **Graham, H**, **Gunther, SH**, **Hamilton, I**, **Hang, Y**, **Hänninen, R**, **Hartinger, S**, **He, K**, **Heidecke, J**, **Hess, JJ**, **Hsu, SC**, **Jamart, L**, **Jankin, S**, **Jay, O**, **Kelman, I**, **Kiesewetter, G**, **Kinney, P**, **Kniveton, D**, **Kouznetsov, R**, **Larosa, F**, **Lee, JKW**, **Lemke, B**, **Liu, Y**, **Liu, Z**, **Lott, M**, **Lotto Batista, M**, **Lowe, R**, **Odhiambo Sewe, M**, **Martinez-Urtaza, J**, **Maslin, M**, **McAllister, L**, **McMichael, C**, **Mi, Z**, **Milner, J**, **Minor, K**, **Minx, JC**, **Mohajeri, N**, **Momen, NC**, **Moradi-Lakeh, M**, **Morrissey, K**, **Munzert, S**, **Murray, KA**, **Neville, T**, **Nilsson, M**, **Obradovich, N**, **O'Hare, MB**, **Oliveira, C**, **Oreszczyn, T**, **Otto, M**, **Owfi, F**, **Pearman, O**, **Pega, F**, **Pershing, A**, **Rabbaniha, M**, **Rickman, J**, **Robinson, EJZ**, **Rocklöv, J**, **Salas, RN**, **Semenza, JC**, **Sherman, JD**, **Shumake-Guillemot, J**, **Silbert, G**, **Sofiev, M**, **Springmann, M**, **Stowell, JD**, **Tabatabaei, M**, **Taylor, J**, **Thompson, R**, **Tonne, C**, **Treskova, M**, **Trinanes, JA**, **Wagner, F**, **Warnecke, L**, **Whitcombe, H**, **Winning, M**, **Wyns, A**, **Yglesias-González, M**, **Zhang, S**, **Zhang, Y**, **Zhu, Q**, **Gong, P**, **Montgomery, H**, **Costello, A.** 2023. The 2023 report of the *Lancet* Countdown on health and climate change: The imperative for a health-centred response in a world facing irreversible harms. *The Lancet* **402**(10419): 2346–2394. DOI: https://doi.org/10.1016/S0140-6736(23)01859-7.

Downloaded from http://online.ucpress.edu/elementa/article-pdf/13/1/00089/895115/elementa.2024.00089.pdf by guest on 29 September 2025

Seiler, W, **Crutzen, PJ.** 1980. Estimates of gross and net fluxes of carbon between the biosphere and atmosphere from biomass burning. *Climatic Change* **2**: 207–247. DOI: https://doi.org/10.1007/BF00137988.

Soares, J, **Sofiev, M**, **Hakkarainen, J.** 2015. Uncertainties of wild-land fires emission in AQMEII phase 2 case study. *Atmospheric Environment* **115**: 361–370. DOI: https://doi.org/10.1016/j.atmosenv.2015.01.068.

Sofiev, M, **Ermakova, T**, **Vankevich, R.** 2012. Evaluation of the smoke-injection height from wild-land fires using remote-sensing data. *Atmospheric Chemistry and Physics* **12**: 1995–2006. DOI: https://doi.org/10.5194/acp-12-1995-2012.

Sofiev, M, **Vankevich, R**, **Ermakova, T**, **Hakkarainen, J.** 2013. Global mapping of maximum emission heights and resulting vertical profiles of wildfire emissions. *Atmospheric Chemistry and Physics* **13**: 7039–7052. DOI: https://doi.org/10.5194/acp-13-7039-2013.

Sofiev, M, **Vankevich, R**, **Lotjonen, M**, **Prank, M**, **Petukhov, V**, **Ermakova, T**, **Koskinen, J**, **Kukkonen, J**. 2009. An operational system for the assimilation of the satellite information on wild-land fires for the needs of air quality modelling and forecasting. *Atmospheric Chemistry and Physics* **9**: 6833–6847. DOI: https://doi.org/10.5194/acp-9-6833-2009.

Soja, AJ, **Al-Saadi, JA**, **Giglio, L**, **Randall, D**, **Kittaka, C**, **Pouliot, GA**, **Kordzi, JJ**, **Raffuse, SM**, **Pace, TG**, **Pierce, T**, **Moore, T**, **Roy, B**, **Pierce, B**, **Szykman, JJ.** 2009. Assessing satellite-based fire data for use in the National Emissions Inventory. *Journal of Applied Remote Sensing* **3**(1): 031504. DOI: https://doi.org/10.1117/1.3148859.

Tang, W, **Emmons, LK**, **Buchholz, RR**, **Wiedinmyer, C**, **Schwantes, RH**, **He, C**, **Kumar, R**, **Pfister, GG**, **Worden, HM**, **Hornbrook, RS**, **Apel, EC.** 2022. Effects of fire diurnal variation and plume rise on U.S. air quality during FIREX-AQ and WE-CAN based on the Multi-Scale Infrastructure for Chemistry and Aerosols (MUSICAv0). *Journal of Geophysical Research: Atmospheres* **127**(16): e2022JD036650. DOI: https://doi.org/10.1029/2022JD036650.

Urbanski, SP, **O'Neill, SM**, **Holder, AL**, **Green, SA**, **Graw, RL.** 2022. Emissions, in Peterson, DL, McCaffrey, SM, Patel-Weynand, T eds., *Wildland fire smoke in the United States*. Cham, Switzerland: Springer. DOI: https://doi.org/10.1007/978-3-030-87045-4_5.

van der Velde, IR, **van der Werf, GR**, **Houweling, S**, **Maasakkers, JD**, **Borsdorff, T**, **Landgraf, J**, **Tol, P**, **van Kempen, TA**, **van Hees, R**, **Hoogeveen, R**, **Veefkind, JP**, **Aben, I.** 2021. Vast CO_2 release from Australian fires in 2019–2020 constrained by satellite. *Nature* **597**: 366–369. DOI: https://doi.org/10.1038/s41586-021-03712-y.

van der Velde, IR, **van der Werf, GR**, **van Wees, D**, **Schutgens, NAJ**, **Vernooij, R**, **Houweling, S**, **Tonucci, E**, **Chuvieco, E**, **Randerson, JT**, **Frey, MM**, **Borsdorff, T**, **Aben, I.** 2024. Small fires, big impact: Evaluating fire emission estimates in Southern Africa using new satellite imagery of burned area and carbon monoxide. *Geophysical Research Letters* **51**: e2023GL106122. DOI: https://doi.org/10.1029/2023GL106122.

van der Werf, GR, **Randerson, JT**, **Giglio, L**, **Collatz, GJ**, **Mu, M**, **Kasibhatla, PS**, **Morton, DC**, **Defries, RS**, **Jin, Y**, **van Leeuwen, TT.** 2010. Global fire emissions and the contribution of deforestation, savanna, forest, agricultural, and peat fires (1997–2009). *Atmospheric Chemistry and Physics Discussions* **10**(6): 16153–16230. DOI: https://doi.org/10.5194/acpd-10-16153-2010.

van der Werf, GR, **Randerson, JT**, **Giglio, L**, **van Leeuwen, TT**, **Chen, Y**, **Rogers, BM**, **Mu, M**, **van Marle, MJE**, **Morton, DC**, **Collatz, GJ**, **Yokelson, RJ**, **Kasibhatla, PS.** 2017. Global fire emissions estimates during 1997–2016. *Earth System Science Data* **9**: 697–720. DOI: https://doi.org/10.5194/essd-9-697-2017.

van Leeuwen, TT, **van der Werf, GR**, **Hoffmann, AA**, **Detmers, RG**, **Rücker, G**, **French, NHF**, **Archibald, S**, **Carvalho JA Jr**, **Cook, GD**, **de Groot, WJ**, **Hély, C**, **Kasischke, ES**, **Kloster, S**, **McCarty, JL**, **Pettinari, ML**, **Savadogo, P**, **Alvarado, EC**, **Boschetti, L**, **Manuri, S**, **Meyer, CP**, **Siegert, F**, **Trollope, LA**, **Trollope, WSW.** 2014. Biomass burning fuel consumption rates: A field measurement database. *Biogeosciences* **11**: 7305–7329. DOI: https://doi.org/10.5194/bg-11-7305-2014.

van Wees, D, **van der Werf, GR**, **Randerson, JT**, **Rogers, BM**, **Chen, Y**, **Veraverbeke, S**, **Giglio, L**, **Morton, DC.** 2022. Global biomass burning fuel consumption and emissions at 500 m spatial resolution based on the Global Fire Emissions Database (GFED). *Geoscientific Model Development* **15**: 8411–8437. DOI: https://doi.org/10.5194/gmd-15-8411-2022.

Vernooij, R, **Eames, T**, **Russell-Smith, J**, **Yates, C**, **Beatty, R**, **Evans, J**, **Edwards, A**, **Ribeiro, N**, **Wooster, M**, **Strydom, T**, **Giongo, MV**, **Borges, MA**, **Menezes Costa, M**, **Barradas, ACS**, **van Wees, D**, **van der Werf, GR.** 2023. Dynamic savanna burning emission factors based on satellite data using a machine learning approach. *Earth System Dynamics* **14**: 1039–1064. DOI: https://doi.org/10.5194/esd-14-1039-2023.

Wang, J, **Ge, C**, **Yang, Z**, **Hyer, EJ**, **Reid, JS**, **Chew, BN**, **Mahmud, M**, **Zhang, Y**, **Zhang, M.** 2013. Mesoscale modeling of smoke transport over the Southeast Asian Maritime Continent: Interplay of sea breeze, trade wind, typhoon, and topography. *Atmospheric Research* **122**: 486–503. DOI: https://doi.org/10.1016/j.atmosres.2012.05.009.

Whaley, CH, **Butler, T**, **Adame, JA**, **Ambulkar, R**, **Arnold, SR**, **Buchholz, RR**, **Gaubert, B**, **Hamilton, DS**, **Huang, M**, **Hung, H**, **Kaiser, JW**, **Kaminski, JW**, **Knote, C**, **Koren, G**, **Kouassi, JL**, **Lin, M**, **Liu, T**, **Ma, J**, **Manomaiphiboon, K**, **Bergas Masso, E**, **McCarty, JL**, **Mertens, M**, **Parrington, M**, **Peiro, H**, **Saxena, P**, **Sonwani, S**, **Surapipith, V**, **Tan, D**,

Downloaded from http://online.ucpress.edu/elementa/article-pdf/13/1/00089/895115/elementa.2024.00089.pdf by guest on 29 September 2025

Tang, W, **Tanpipat, V**, **Tsigaridis, K**, **Wiedinmyer, C**, **Wild, O**, **Xie, Y**, **Zuidema, P.** 2025. HTAP3 Fires: Towards a multi-model, multi-pollutant study of fire impacts. *Geoscientific Model Development Discussions* [preprint]. DOI: https://doi.org/10.5194/gmd-2024-126.

Wiedinmyer, C, **Akagi, SK**, **Yokelson, RJ**, **Emmons, LK**, **Al-Saadi, JA**, **Orlando, JJ**, **Soja, AJ.** 2011. The Fire INventory from NCAR (FINN): A high resolution global model to estimate the emissions from open burning. *Geoscientific Model Development* **4**: 625–641. DOI: https://doi.org/10.5194/gmd-4-625-2011.

Wiedinmyer, C, **Emmons, L.** 2022. Fire Inventory from NCAR version 2 Fire Emission. Research Data Archive at the National Center for Atmospheric Research. Computational and Information Systems Laboratory. DOI: https://doi.org/10.5065/XNPA-AF09.

Wiedinmyer, C, **Kimura, Y**, **McDonald-Buller, EC**, **Emmons, LK**, **Buchholz, RR**, **Tang, W**, **Seto, K**, **Joseph, MB**, **Barsanti, KC**, **Carlton, AG**, **Yokelson, R.** 2023. The Fire Inventory from NCAR version 2.5: An updated global fire emissions model for climate and chemistry applications. *Geoscientific Model Development* **16**: 3873–3891. DOI: https://doi.org/10.5194/gmd-16-3873-2023.

Wooster, MJ, **Roberts, G**, **Freeborn, PH**, **Xu, W**, **Govaerts, Y**, **Beeby, R**, **He, J**, **Lattanzio, A**, **Fisher, D**, **Mullen, R.** 2015. LSA SAF Meteosat FRP products—Part 1: Algorithms, product contents, and analysis. *Atmospheric Chemistry and Physics* **15**: 13217–13239. DOI: https://doi.org/10.5194/acp-15-13217-2015.

Wooster, MJ, **Roberts, G**, **Perry, GLW**, **Kaufman, YJ.** 2005. Retrieval of biomass combustion rates and totals from fire radiative power observations: FRP derivation and calibration relationships between biomass consumption and fire radiative energy release. *Journal of Geophysical Research: Atmospheres* **110**: D24311. DOI: https://doi.org/10.1029/2005JD006318.

Xu, J, **Morris, PJ**, **Liu, J**, **Holden, J.** 2018. PEATMAP: Refining estimates of global peatland distribution based on a meta-analysis. *CATENA* **160**: 134–140. DOI: https://doi.org/10.1016/J.CATENA.2017.09.010.

Yokelson, RJ, **Burling, IR**, **Gilman, JB**, **Warneke, C**, **Stockwell, CE**, **de Gouw, J**, **Akagi, SK**, **Urbanski, SP**, **Veres, P**, **Roberts, JM**, **Kuster, WC**, **Reardon, J**, **Griffith, DWT**, **Johnson, TJ**, **Hosseini, S**, **Miller, JW**, **Cocker, DR III**, **Jung, H**, **Weise, DR.** 2013. Coupling field and laboratory measurements to estimate the emission factors of identified and unidentified trace gases for prescribed fires. *Atmospheric Chemistry and Physics* **13**: 89–116. DOI: https://doi.org/10.5194/acp-13-89-2013.

Yokelson, RJ, **Griffith, DWT**, **Ward, DE.** 1996. Open-path Fourier transform infrared studies of large-scale laboratory biomass fires. *Journal of Geophysical Research: Atmospheres* **101**: D15. DOI: https://doi.org/10.1029/96JD01800.

Zhang, L, **Montuoro, R**, **McKeen, SA**, **Baker, B**, **Bhattacharjee, PS**, **Grell, GA**, **Henderson, J**, **Pan, L**, **Frost, GJ**, **McQueen, J**, **Saylor, R**, **Li, H**, **Ahmadov, R**, **Wang, J**, **Stajner, I**, **Kondragunta, S**, **Zhang, X**, **Li, F.** 2022. Development and evaluation of the Aerosol Forecast Member in the National Center for Environment Prediction (NCEP)'s Global Ensemble Forecast System (GEFS-Aerosols v1). *Geoscientific Model Development* **15**: 5337–5369. DOI: https://doi.org/10.5194/gmd-15-5337-2022.

Zheng, B, **Ciais, P**, **Chevallier, F**, **Yang, H**, **Canadell, JG**, **Chen, Y**, **van der Velde, IR**, **Aben, I**, **Chuvieco, E**, **Davis, SJ**, **Deeter, M**, **Hong, C**, **Kong, Y**, **Li, H**, **Li, H**, **Lin, X**, **He, K**, **Zhang, Q.** 2023. Record-high CO_2 emissions from boreal fires in 2021. *Science* **379**(6635): 912–917. DOI: https://doi.org/10.1126/science.ade0805.

Zhou, M, **Wang, J**, **Garcia, LC**, **Chen, X**, **da Silva, AM**, **Wang, Z**, **Román, MO**, **Hyer, EJ**, **Miller, SD.** 2023. Enhancement of nighttime fire detection and combustion efficiency characterization using Suomi-NPP and NOAA-20 VIIRS instruments. *IEEE Transactions on Geoscience and Remote Sensing* **61**: 1–20. DOI: https://doi.org/10.1109/TGRS.2023.3261664.

Downloaded from http://online.ucpress.edu/elementa/article-pdf/13/1/00089/895115/elementa.2024.00089.pdf by guest on 29 September 2025

Downloaded from http://online.ucpress.edu/elementa/article-pdf/13/1/00089/895115/elementa.2024.00089.pdf by guest on 29 September 2025

How to cite this article: Parrington, M, Whaley, CH, French, NHF, Buchholz, RR, Pan, X, Wiedinmyer, C, Hyer, EJ, Kondragunta, S, Kaiser, JW, Di Tomaso, E, van der Werf, GR, Sofiev, M, Barsanti, KC, da Silva, AM, Darmenov, AS, Tang, W, Griffin, D, Desservettaz, M, Carter, T, Paton-Walsh, C, Liu, T, Uppstu, A, Palamarchuk, J. 2025. Biomass burning emission estimation in the MODIS era: State-of-the-art and future directions. *Elementa: Science of the Anthropocene* 13(1). DOI: https://doi.org/10.1525/elementa.2024.00089

Domain Editor-in-Chief: Detlev Helmig, Boulder AIR LLC, Boulder, CO, USA

Associate Editor: Maria Val Martin, School of Biosciences, The University of Sheffield, Sheffield, UK

Knowledge Domain: Atmospheric Science

Part of an Elementa Special Feature: International Global Atmospheric Chemistry (IGAC) 35-year Anniversary

Published: September 04, 2025 **Accepted:** June 7, 2025 **Submitted:** December 3, 2024

Copyright: © 2025 The Author(s). This is an open-access article distributed under the terms of the Creative Commons Attribution 4.0 International License (CC-BY 4.0), which permits unrestricted use, distribution, and reproduction in any medium, provided the original author and source are credited. See http://creativecommons.org/licenses/by/4.0/.

ELEMENTA Science of the Anthropocene

Elem Sci Anth is a peer-reviewed open access journal published by University of California Press.

OPEN ACCESS